Interaction between high-energy particles and nuclei

Yu. P. Nikitin, I. L. Rozental', and F. M. Sergeev

Moscow Engineering Physics Institute
and Institute of Space Research, USSR Academy of Sciences
Usp. Fiz. Nauk **121** 3–53 (January 1977)

A review is given of the results of experimental studies of interactions between high-energy particles ($E_0 \gtrsim 20$GeV) and nuclei. It is emphasized that experiment shows a very weak dependence of many of the important parameters of multiple production on the number of nucleons in the nucleus. Observed phenomena can be understood either within the framework of the hydrodynamic (classical) approach or within the framework of the quantum-mechanical, field-theoretical approach (parton model). Suggestions are outlined for further studies that might throw light on the mechanism of space-time development of the interaction processes. The references cover the period up to May 1, 1976.

PACS numbers: 13.85.Hd, 12.40.Cc

CONTENTS

INTRODUCTION

Cosmic-ray and accelerator experiments performed in the course of the last few decades have demonstrated a very striking property of interactions between high-energy particles and atomic nuclei.

Specifically, if we confine our attention to hadrons formed during the collision time, we find that their parameters exhibit a very weak dependence on the mass number A of the target nucleus, which is at rest in the laboratory frame (L system), and on the type of incident particle.[1)] For a given energy release in the center-of-mass frame (C system) of the colliding particles, the distribution of secondary particles with respect to multiplicity, the invariant cross section $Ed^3\sigma/dp^3$, the rapidity distribution dn/dy, the distribution over the transverse momenta $dn/dp_\perp$, and the abundance of the resulting hadrons are very weakly dependent on A and on the type of incident particle. Occasionally, to within experimental error, there is no dependence at all. Examination of the primary-particle parameters indicates that the inelasticity coefficient shows a weak dependence on A when the primary particle is a hadron.

We note at once that we shall confine our attention to primary-particle energies greater than or of the order of $E_0 \gtrsim 20$–30 GeV, where E_0 is the energy in the L system.

Unfortunately, the volume of experimental data available at such high energies is as yet insufficient to enable us to derive unambiguous conclusions. This limitation is particularly characteristic for processes involving the participation of leptons. There are two reasons for this. Firstly, there are the methodological difficulties of studying interactions with nuclei (see[1], Chap. 1) and, secondly, collisions with nuclei have tended to be neglected because they involve a process that is more complicated than a collision between two hadrons. The simple logic of this argument is that one tries to achieve an understanding of the simpler phenomenon, namely, the collision between two hadrons, and then proceeds to more complex processes. This argument is valid, in general, but can hardly be justified in the present context. Thus, we note, first of all, that our level of understanding of multiple processes occurring during collisions between two hadrons is quite high.[2] In fact, the theory of multiple processes has now crystallized and has been reasonably rigorously formulated in its general outline. On the other hand, studies of collisions with nuclei have posed the clear question as to the reason for the above weak dependence on the mass number. If we attempt to provide a rough formulation of the basic problem of multiple processes (we shall return to this question in Chap. 2), we find that it reduces to the question of the description of the virtual phase. At present, the two main approaches, i.e., multiperipheral and statistical-hydrodynamic, suggest that this phase has a finite (nonzero) space-time size. From the standpoint of the quantum-mechanical approach (multiperipheralism), this phase is described by diagrams; in the classical description, it is reduced to statistical

[1)]We shall assume that the dependence is weak if it is of the form $\sim A^\alpha$ with $\alpha \ll 2/3$. We recall that $A^{2/3}$ represents the geometric cross section.

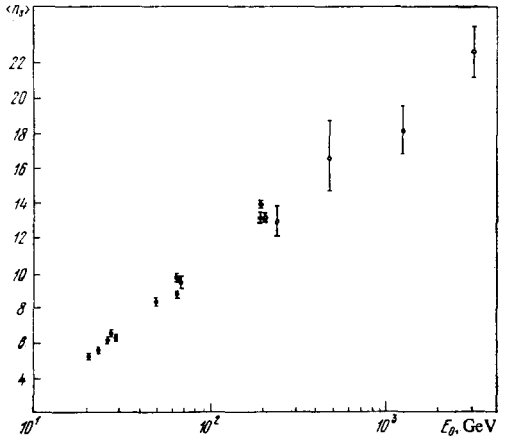

FIG. 1. Energy dependence of $\langle n_s \rangle$ in emulsion.[6,22]

hydrodynamics.

These two approaches are considered in detail in Chap. 2. Here, we confine ourselves to a brief announcement. Its aim is to facilitate the understanding of certain diagrams representing simultaneously both experimental data and their theoretical interpretation.

The classical approach reduces to the formation of a cluster which does not include the leading particle (Secs. 2.6 and 2.8).

In the parton version of the multiperipheral model (Sec. 2.9), a fast hadron dissociates into partons during the time of the virtual phase. Partons of high energy (but short wavelength) freely leave the nucleus and then assemble again into hadrons. The interaction is executed by low-energy partons. The nucleus is an object of large spatial size which increases with the number A of nucleons in the nucleus. One might therefore reasonably expect that detailed studies of interactions with nuclei will facilitate the elucidation of the space-time development of the process. Here, we have to distinguish two axes, i.e., the longitudinal and the transverse. In processes developing in the longitudinal direction, we see manifestations of the properties of hydronic material, whereas processes developing in the transverse direction depend on the properties of nuclear matter (see Sec. 2.1).

It is already clear that experimental data obtained by studying collisions occurring at high energies (weak dependence of parameters on A) are in conflict with the description involving successive collisions between the incident particle and the quasifree nucleons in the nucleus. If this were not so (see Sec. 2.5), the dependence on A should be strong. Experimental data indicate the essential validity of the above theoretical approaches. On the other hand, the possible universal character of interactions of leptons and hadrons may be an indication that the final phase of multiple processes plays a determining role, and this imposes an essential restriction on the possible range of theoretical models.

We note one further important feature of interactions with nuclei. At energies $E_0 \gtrsim 100$ GeV, some of the parameters of multiple processes cease to depend on E_0. This we shall refer to as the asymptotic state. The aim of the present paper is to review existing information on interactions between high-energy particles and nuclei, and to formulate certain problems that can be usefully solved in this part of physics.

1. EXPERIMENTAL STUDIES OF INTERACTIONS BETWEEN HIGH-ENERGY PARTICLES AND NUCLEI

In this section, we review some of the experimental results on multiple production during interactions of hadrons and leptons with nuclei. Lack of space prevents our examining in detail the very diverse experimental material. Partial justification for this is provided by the fact that there are published reviews (for example, [3,4]) and monographs[5,6] in which these questions are reviewed up to 1972. We have confined ourselves largely to new experimental data on interactions with nuclei at primary energies $E_0 \gtrsim 20$ GeV, and have paid particular attention to the asymptotic properties of the multiple production process which begin to manifest themselves at such energies. In selecting the experimental data for review, we tried to emphasize those data which, at least in our view, provide a good illustration of the basic problem in the interaction between elementary particles and nuclei, namely, the weak dependence of many of the parameters on the mass number A.

1.1. Multiplicity of secondary particles

The multiplicity of secondary hadrons in the final state state is an important criterion for verifying the predictions of theoretical models.

In the ensuing review, the products of a nuclear interaction will be classified in terms of the notation adopted in the analysis of data obtained with nuclear emulsions. The multiplicities will be designated as follows: shower particles n_s ($\beta > 0.7$), strongly ionizing particles N_h ($\beta < 0.7$), gray tracks n_g (mainly protons), and black tracks n_b ($N_h = n_g + n_b$).

Experimental data on multiplicity at present cover primary-particle energies up to ~10 TeV. In this section, we consider the data that characterize certain definite features in the behavior of n_s as a function of the primary energy E_0 and the mass number A of the target nucleus.

The mean value $\langle n_s \rangle$ increases monotonically with increasing primary energy. It increases by a factor of two between primary energies of about 20 and 200 GeV (Fig. 1 and Table I). At higher energies, the rate of increase of $\langle n_s \rangle$ is lower. The role of the target nucleus in the development of the multiple production process becomes more obvious if we consider the ratio $R_A = \langle n_s \rangle / \langle n_s \rangle_H$, where $\langle n_s \rangle_H$ is the mean multiplicity of shower particles during the collision between a hadron and a nucleon at the same primary energy E_0. The ratio R_A is sometimes referred to as the normalized mean multiplicity.

Figure 2a shows R_A for an emulsion ($A \sim 65$) as a function of E_0. These data are taken from[7]. It is clear that the experimental data are not inconsistent with the

TABLE I. a) Mean multiplicities at different energies (photographic emulsion data)

Primary momentum p_0, GeV/c	$\langle n \rangle$	Light nuclei	CNO	AgBr	All nuclei	Ref.
π^-, 17, emulsion	n_s	4.2±0.4	4.1±0.4	5.7±0.3	5.3±0.3	17
	n_g	0.6±0.1	0.45±0.04	2.0±0.3	1.5±0.2	
	n_b	2.9±0.3	1.9±0.3	6.5±0.4	5.0±0.4	
π^-, 17.5, emulsion	n_s			6.7±0.2		18
	n_g			3.7±0.2		
	n_b			7.8±0.2		
	N_h			11.5±0.5		
π, 40, emulsion	n_s			6.98±0.04		33
π, 60, emulsion	n_s	8.0±0.6	7.4±0.5	9.3±0.2		17
	n_g	1.0±0.2	0.78±0.06	3.2±0.1	2.6±0.2	
	n_b	2.6±0.2	1.9±0.1	5.8±0.2	4.7±0.2	
π, 60, emulsion	n_s			9.9±0.2	9.23±0.07	18
	n_g			3.8±0.2		
	n_b			7.8±0.2		
	N_h			11.6±0.3	7.02±0.05	
p, 21, emulsion	n_s	5.4±0.4	4.1±0.3	6.2±0.2	5.8±0.2	17
	n_g	0.9±0.1	0.7±0.1	3.9±0.2	2.9±0.2	
	n_b	2.7±0.2	2.2±0.1	5.9±0.3	4.6±0.2	
p, 21.5, emulsion	n_s				6.28±0.11	21
p, 60, emulsion	n_s	6.7±0.4	6.4±0.5	8.9±0.5		17
	n_g	0.8±0.1	0.63±0.07	3.4±0.2		
	n_b	2.7±0.1	2.0±0.2	4.9±0.6		
p, 67, emulsion	n_s	6.7±0.6	6.3±0.7	10.1±0.4	8.8±0.3	17
	n_g	0.8±0.1	0.6±0.1	3.4±0.2	2.5±0.1	
	n_b	2.4±0.1	1.5±0.1	6.2±0.3	4.7±0.2	
p, 67, emulsion	n_s			10.7±0.3		18
	n_g			3.7±0.2		
	n_b			7.6±0.3		
	N_h			11.3±0.3		
p, 69, emulsion	n_s				11.08±0.18	21
p, 200, emulsion	n_s		11.0±0.3	15.4±0.3	14.53±0.22	21, 22
					13.9±0.2	
	n_g		0.90±0.05	3.29±0.10	2.48±0.08	
	n_b		1.80±0.08	6.36±0.16	4.79±0.12	
	N_h		2.61±0.08	9.92±0.17	7.40±0.13	
			2.70±0.11	9.66±0.24	7.26±0.19	
p, 300, emulsion	n_s				16.0±1.5	9

b) Mean multiplicity of relativistic particles as a function of energy.

Target nucleus	Primary momentum, GeV/c	$\langle n_s \rangle$	Ref.	Target nucleus	Primary momentum, GeV/c	$\langle n_s \rangle$	Ref.
CH_2	p, 70	6.6±0.6	10	Al	~600	12.0±0.7	10
	170	7.7±0.5		Fe	p, 160	12.25±0.89	
	600	9.7±0.6			260	13.21±1.16	10
C	π, 40	6.36±0.06	8		520	16.05±2.90	
	p, 85	7.89±0.34	13	Cu	p, 70	8.0±0.6	
C	120	10.13±0.42	13		170	12.2±1.1	10
	173	11.44±0.64			~600	15.7±1.3	
	379	12.28±0.83		Sn	p, 160	13.31±1.13	
Al	p, 70	8.1±0.4	10		260	15.14±1.40	13
	160	11.25±0.76	13		520	17.05±3.60	
	170	10.1±0.6	10	Pb	p, 160	14.75±1.41	13
	260	12.87±1.18	13		260	15.61±1.51	
	520	14.0±2.49					

very important conclusion that R_A is independent of energy for $E_0 \gtrsim 70$ GeV. The limiting value of R_A for an emulsion is close to 1.7. There is experimental evidence for the fact that the asymptotic behavior sets in earlier for light nuclei than for heavy nuclei.[8]

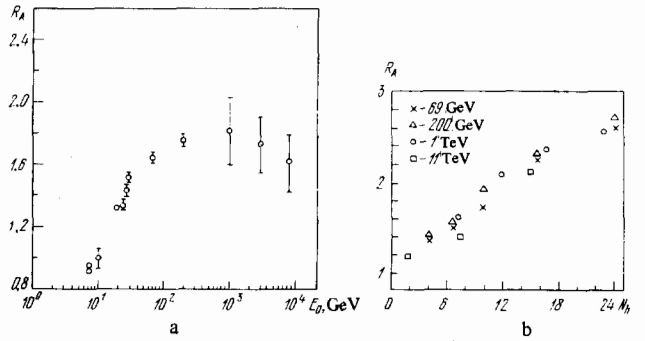

FIG. 2. a) Energy dependence of $R_A = \langle n_s \rangle / \langle n_s \rangle_H$ for emulsion nuclei;[7] b) dependence of $R_A = \langle n_s(E_0) \rangle / \langle n_s(E_0) \rangle_H$ on the number N_h of highly ionizing particles in a star. Photoemission data taken from[20].

TABLE II.

E_0, GeV	c	d	γ	R_A	α
6.2	0.91±0.03	0.09±0.03	0.72±0.048	1.27±0.02	0.05
~21.0	0.82±0.03	0.18±0.03	0.46±0.17	1.54±0.03	0.10
27.0	0.75±0.04	0.25±0.04	0.60±0.24	1.61±0.03	0.13
67.0	0.74±0.03	0.26±0.02	0.35±0.10	1.80±0.05	0.14
200.0	0.70±0.02	0.30±0.02	0.31±0.08	1.87±0.03	0.15
~1000	0.74	0.26	—	1.79±0.26	—
~3000	0.74±0.17	0.31±0.06	0.18±0.25	1.88±0.30	0.17

Here and henceforth, the phrase "asymptotic behavior" will be used to indicate the tendency of a physical quantity toward a simple functional dependence (in particular, a constant) above a certain value of the primary energy E_0.

An important property of the ratio R_A is that it is a slowly-varying function of the mass number of the target nucleus. If we suppose that $R_A = A^\alpha$, then it turns out that α increases from 0 at $E_0 = 10$ GeV to about 0.12 at 68 GeV. At primary energies above 200 GeV, the exponent α remains practically constant ($\alpha = 0.13$–0.15).[7,9] According to[7], $\alpha = 0.131 \pm 0.005$ when $E_0 = 200$ GeV.

The weak dependence of α on the mass number has been confirmed by cosmic-ray studies[10] in which R_A was represented by $R_A = \beta A^{1/3}$. For Al, Cu, Ag, and Br, and energies in the range 50–3000 GeV, the experimental data can be described by this formula (see also[14]) with $\beta = 0.41 \pm 0.04$. If we suppose that $\beta = 1$, then it again turns out that $R_A \sim A^{0.1}$.

In general, the exponent α is very dependent on the type of approximation used for R_A.

The linear dependence of R_A on $A^{1/3}$ has been analyzed in detail in[12] using nuclear-emulsion data for protons with primary energies between 6.2 and 3000 GeV. Analysis shows that the experimental data can be described by the formula $R_A = c + dA^{1/3}$, where c and d (and, consequently, R_A) are independent of the primary energy for $E_0 \gtrsim 50$ GeV. Using this result and the data for $E_0 = 67$ GeV and $E_0 = 200$ GeV, Babecki[15] showed that $c = 0.716 \pm 0.018$ and $d = 0.283 \pm 0.015$. He also considered the possible parametrization of the more general expression $R_A = c + dA^\gamma$. Data for $A = 1$, 14, and 95 were used and the results are summarized in Table II. The last column of Table II gives the values of α in the formula $R_A = \beta A^\alpha$ (the coefficient was also varied). It is clear that the value of α remains very small (~0.1–0.2) in a broad range of primary energies E_0 (see Secs. 2.6 and 2.9).

Experimental data obtained for particular nuclei are of particular interest for studies of the dependence of R_A on the mass number. Vishvanath and Bussian[13] have investigated multiple production on C, Al, Fe, Sn, and Pb at primary energies between about 80 and about 600 GeV. The experiment was carried out in cosmic rays in which the primary flux consisted of about 70% protons and about 30% pions. The dependence of R_A on the mass number, obtained at about 160 GeV, is shown

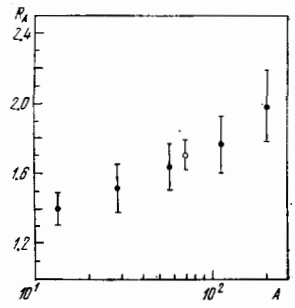

FIG. 3. Mean normalized multiplicity of shower particles as a function of mass number A.[13] Open circle represents emulsion data.

in Fig. 3. When these data are approximated by $R_A = A^{\alpha}$, it is found that $\alpha = 0.129 \pm 0.004$. Thus, to within the limits of statistical precision, the quantity $R_A(\alpha)$ turns out to be independent of primary energy for $E_0 \gtrsim 160$ GeV.

The dependence of R_A on A in the case of pions interacting with C, Al, Cu, Ag, Pb, and U was obtained in[14] for two values of E_0, namely, 100 and 175 GeV. Comparison shows that, for a given value of A, the quantity R_A for primary pions is somewhat lower than for primary protons. However, both data can be described by a single formula if they are represented as functions of the quantity $\nu = A\sigma_N/\sigma_t$, where σ_N and σ_t are the inelastic cross sections for a hadron on a nucleon and a nucleus, respectively. The quantity ν represents the mean number of collisions between the primary hadron and nucleons in the nuclear interior. The dependence of R_A on ν turns out to be almost linear. It is noted in[15] that this fact confirms the expression $R_A = c + dA^{1/3}$ since $\sigma_t \sim A^{0.7}$ (see Sec. 1.4).

Thus, we must emphasize once again that R_A and, consequently, the mean multiplicity $\langle n_s \rangle$ as well, are slowly-varying functions of the mass number A of the target nucleus.

The multiplicity distribution can be characterized by the values of its moments. The variance $D = \langle n_s \rangle^2 - \langle n^2 \rangle_s$ (second central moment) of the distribution in hadron-nucleus collisions behaves itself as a function of n_s in the same way as the variance of the distribution of multiplicity in hadron-nucleon collisions. Figure 4a shows the experimental results for $\sqrt{D}(\langle n \rangle_s)$ obtained with nuclear emulsions.[7] To within experimental error, there is a linear relationship between $\sqrt{D}$ and n_s. This is similar to the result obtained for pp interactions, namely, $\sqrt{D} = a\langle n_s \rangle + b$, where a turns out to be close to the value $a_{pp} \approx 0.6$. Thus, for all the interactions considered in[7], it turns out that $a = 0.64 \pm 0.02$. Figure 4b shows the function $M = \langle n_s \rangle / \sqrt{D}$ for a number of nuclei at different energies E_0.[10] In all cases, this ratio turns out to be close to 2 (as in pp collisions) and is practically independent of E_0. These properties indicate in particular that n_s does not follow the Poisson distribution for which one would expect $M \sim \sqrt{\langle n_s \rangle}$.

The similarity with elementary collisions can also be seen in the distribution of the probability for the production of n fast particles, $W(n) = \sigma_n/\sigma_t$, where σ_n is the production cross section for a star with n fast particles. It is well known that, in hadron-nucleon collisions at primary energies of about 50 GeV, this distribution has a universal character, i.e., $\langle n \rangle W(n) = \psi(\xi)$, where $\xi = n/\langle n \rangle$ (this is the KNO scaling put forward in[16]). The verification of this property for hadron-nucleon collisions at high primary energies has been reported by a number of workers (see, for example,[8,9,17-19]). The general conclusion is that there is a universal relationship of the form $\langle n \rangle W(n) = \psi(\xi)$ although there is some disagreement about the precise form of the function $\psi(\xi)$.

It is now clear that the final solution of the problem as to what is the precise form of the nuclear scaling function $\psi(\xi)$ will require a substantial increase in the statistical data obtained for different nuclei. The existence of a nuclear KNO scaling can be regarded as experimentally verified, in principle. The above-mentioned linear dependence of the standard deviation $\sqrt{\langle n_s \rangle^2 - \langle n_s^2 \rangle}$ on n_s is a consequence of the universality of $\psi(\xi)$.

Here, it is also important to note the following. The observed similarity between the elementary and nuclear distribution $\psi(\xi)$ may indicate that a large fraction of the products of multiple production propagates in the nucleus as one whole with a mean free path comparable with the nuclear size.

1.2. Angular distributions of secondary hadrons

The angular distributions exhibit characteristic limiting properties that are directly determined by the dynamics of the hadron-nucleus interaction and have a relatively weak dependence on A. Analysis of the experimental angular distributions of shower particles shows that, in the laboratory frame (L system), there is a narrow cone of angle $\theta_L \approx 0.1 - 0.05$ (it is roughly equal to half the cone angle in the elementary event)

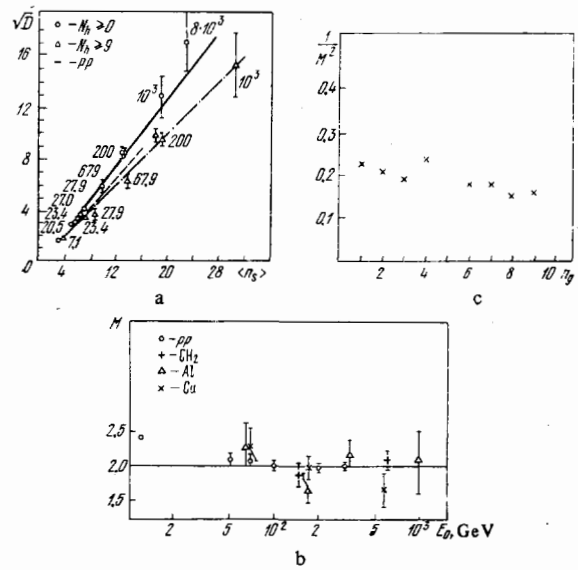

FIG. 4. a) The variance $D = \langle n_s \rangle^2 - \langle n_s^2 \rangle$ as a function of the mean multiplicity of shower particles $\langle n_s \rangle$ (emulsion data); b) energy dependence of $M = \langle n_s \rangle / \sqrt{D}$[10]; c) dependence of M on the number of gray tracks in a star for interactions with heavy nuclei in emulsion ($N_h \geq 7$); primary energy 200 GeV.

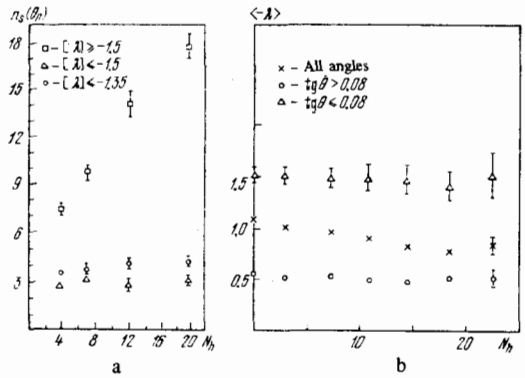

FIG. 5. (a) Mean multiplicity of shower particles as a function of N_h in different angular intervals[20]; b) mean pseudorapidity $\langle -\lambda \rangle = \langle -\log\tan\theta_L \rangle$ as a function of N_h in different angular intervals.[23]

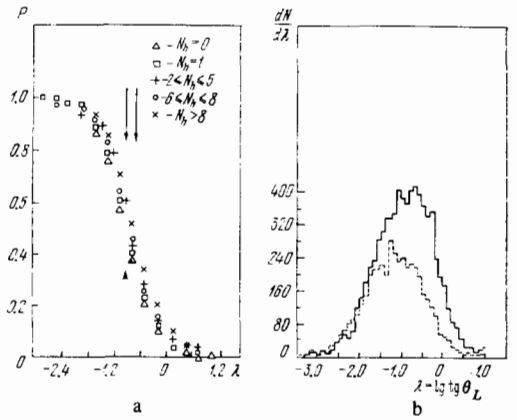

FIG. 6. Distribution of pseudorapidities for interactions between protons and emulsion nuclei at $E_0 = 200$ GeV. a) Integrated (normalized)[23] ($P \geq \lambda$); b) differential for events with $N_h \geq 0$ (solid histogram) and for pp interactions (broken curve). Normalized to the number of interactions.[22]

around the direction of motion of the primary particle in which there is no external manifestation of the effect of the nuclear medium on secondary hadrons. Figure 5a shows the mean multiplicity of shower particles, $\langle n_s \rangle$, as a function of the number N_h of tracks with a high ionization in different angular intervals, deduced from data obtained when photographic emulsions were exposed to protons with momenta of 200 GeV/c.[20] It is clear that the multiplicity of particles produced within the internal cone (laboratory angle of emission $\theta_L \lesssim 0.1$) is not very sensitive to the quantity N_h which is a measure of the excitation of the nucleus [see (2.9)]. The nucleus behaves as if it were transparent to particles within the internal cone, and the overall rise in multiplicity turns out to be localized preferentially in the external cone (laboratory angles of emission $\theta_L \gtrsim 0.1$).

This property is also illustrated in Fig. 6, which shows the angular distribution of relativistic secondary charged particles with $\lambda = \log\tan\theta_L$ as the independent variable (the pseudorapidity λ is approximately equal to the rapidity y in the description of inclusive processes; see[2]).[2)] The data were obtained by exposing emulsions to protons with momenta of 200 GeV/c.[22,23] For comparison, we show the angular distribution of shower particles from pp interactions. For pseudorapidity $\lambda \lesssim -2$, the two distributions are practically identical, and this region may be associated with the fragmentation of the incident particle. Its size along the λ axis is approximately equal to unity, and has a surprising lack of dependence on the primary energy E_0 (see also Sec. 1.3).

Another important fact is that, as the population of the external cone increases, the shape of the angular distribution of particles within the cone is practically unaltered. This conclusion is confirmed by Fig. 5b which shows the mean value $\langle -\lambda \rangle = \langle -\log\tan\theta_L \rangle$ as a function of N_h in the internal and external cones.[23] For $\tan\theta_L = 0.08$, the value of $\langle \lambda \rangle$ in the external cone is constant although the quantity $\langle n_s \rangle$ itself increases with increasing N_h. The small effect of the degree of excitation of the target nucleus on the angular distribution of shower particles can also be seen in the integrated distribution $\langle n_s \rangle$ as a function of the pseudorapidity $\lambda = \log\tan\theta_L$ (see Fig. 6a). The arrows show the values of pseudorapidity dividing the total multiplicity in half. It is clear that the median pseudorapidities corresponding to different values of N_h are roughly the same, and this confirms the weak dependence of the shape of the angular distributions on N_h. The development of the process inside the nucleus, which is accompanied by an increase in N_h, is indicated by the fact that the multiplication tends to shift toward positive pseudo-rapidities, which corresponds to the target fragmentation region.

The dependence of the angular distributions on the primary energy E_0 is shown in Fig. 7, where the distributions are plotted with the values of $\eta = -\ln\tan(\theta_L/2)$ given along the ordinate axis. The figure also shows the results of calculations based on the hydrodynamic model[24] (see Sec. 2.6). It may be concluded that the target-fragmentation region is fully formed for energies $E_0 \gtrsim 50$ GeV. It is clear that, as the primary energy increases, the development of the process is largely dependent on the fragmentation of the incident particle. This ensures that the normalized multiplicity R_A is in-

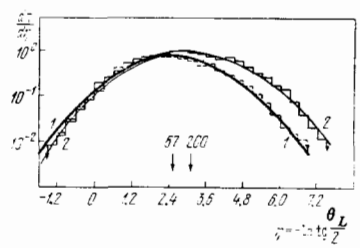

FIG. 7. Distribution of $dn_s/d\eta$ for collisions between protons and emulsion nuclei at primary energies of 67 and 200 GeV (solid histogram—$E_0 = 200$ GeV). Arrows show the positions of the centers of gravity during collision with the mean tube. Solid curve—calculated from hydrodynamic theory.[24]

[2)]We note that there is no generally accepted notation for pseudorapidity. We have used the notation employed in the original paper.

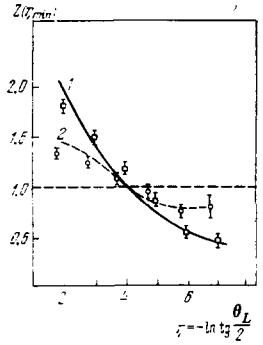

FIG. 8. Dependence of the quantity $Z = \int_{\eta_{min}}^{\infty} F(\eta)\, d\eta / \int_{\eta_{min}}^{\infty} F_0(\eta)\, d\eta$ on the pseudorapidity $\eta = -\ln\tan(\theta_L/2)$. The functions $F_0(\eta)$ and $F(\eta)$ are the distributions for pN and pA interactions in emulsions ($E_0 = 200$ GeV).[31] 1—Interactions with heavy nuclei ($N_h \geq 7$), 2—interactions with light nuclei ($1 \leq N_h \leq 6$), $n_b \geq 1$ with range $R_b \leq 80$. Solid curves—calculation.[27]

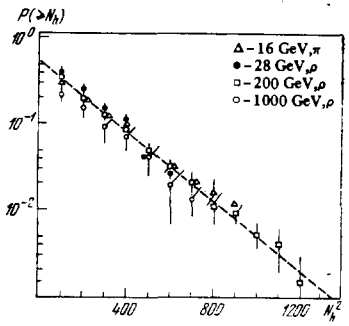

FIG. 10. Probability of appearance of stars in emulsion with number of highly ionizing tracks greater than N_h.[23]

dependent of energy (see Secs. 1.1 and 1.3). In general, one would expect that R_A would fall slightly with increasing E_0, and this is not inconsistent with the experimental results (see Fig. 2a).

When the angular distributions of secondary relativistic particles are investigated, it is convenient to use the variable $Z = \langle n_s(>\eta)\rangle_A / \langle n_s(>\eta)\rangle_H$, which is the ratio of the integrated number of shower particles with pseudorapidity greater than $\eta = -\ln\tan(\theta_L/2)$, obtained for hadron-nucleus interactions, and the integrated number of shower particles with the same pseudorapidity and originating in hadron-proton interactions. This quantity was first considered in[26,35].

The experimental distribution over Z, obtained in[25], is shown in Fig. 8. The solid curves were calculated from the model given in[27] and, as can be seen, the calculations are in agreement with experiment.

The angular distributions (distributions over pseudorapidity) show a definite regularity with $\xi_s = n_s/\langle n_s\rangle$. The distributions of the normalized quantity $(1/\pi\sigma_n)d\sigma_n/d\eta$ for two values of primary energy (30 and 200 GeV) and three intervals of values of this quantity were investigated in[28]. The data show that there is an analogy with the results for pp interactions in that the nuclear data exhibit a peculiar saturation of the angular distribution, i.e., a scaling in ξ_s, which occurs both for the target-fragmentation region and for the incident-particle fragmentation region.

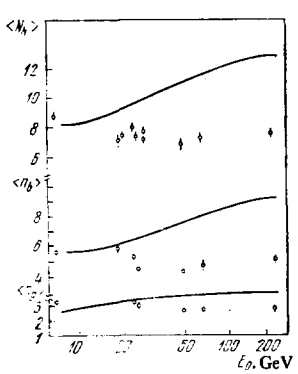

FIG. 9. Energy dependence of $\langle N_h\rangle$, $\langle n_b\rangle$, and $\langle n_g\rangle$.[22] Curves—calculation based on cascade-evaporation model.

mentation region.

1.3. Fragmentation of the target nucleus. Correlations between secondary particles

The fragments of the nuclear target are characterized by the quantities N_h, n_b, and n_g.

The mean multiplicity of strongly ionizing particles, $\langle N_h\rangle$, passes through a maximum near the primary energy of $E_0 \sim 10$ GeV and then decreases at a reducing rate. For $E_0 \gtrsim 20$ GeV, it reaches a constant value of $N_h \approx 7$–8 (Fig. 9 and Table I; see Sec. 2.9). For comparison, the figure also shows the results of calculations based on the intranuclear cascade model (see Sec. 2.5).

The differential distributions of N_h, n_g, and n_b retain the above stability with respect to E_0. The "saturation" of the distributions is manifested, for example, in the integrated probability of the appearance of stars with the number of highly ionized tracks greater than N_h [$P(\gtrsim N_h)$][23] (Fig. 10). This property is also exhibited by the n_g and n_b distributions[22] (see Sec. 2.9).

The differential distribution of identified protons from pion-carbon interactions at primary energies between 4 and 40 GeV was analyzed in[8]. It was shown that, even at these energies, the distribution of protons does not vary to within statistical error.

Whilst for primary energies in excess of about 20 GeV there is an apparent absence of a dependence of the multiplicity of highly ionizing particles on primary energy, the dependence on the geometric size of the nucleus for such particles turns out to be very strong. The multiplicity was investigated in[22] as a function of the mass number of the target nucleus, assuming that it was of the form $\sim A^{\alpha}$. The values of α for dense and gray tracks and for their sum were found to be as follows: $\alpha_b = 0.655 \pm 0.025$; $\alpha_g = 0.672 \pm 0.030$; $\alpha_h = 0.661 \pm 0.025$. It is important to note that the uncertainties indicated against these results do not take into account the precision with which the light and heavy nuclei were separated out in the emulsion. Thus, very approximately, $\langle N_h\rangle$, $\langle n_b\rangle$, $\langle n_g\rangle \sim A^{2/3}$.

The quantities N_h, n_b, and n_g which, as already noted, measure the response of the nucleus to the perturbation imposed upon it, are correlated with the parameters of relativistic particles.

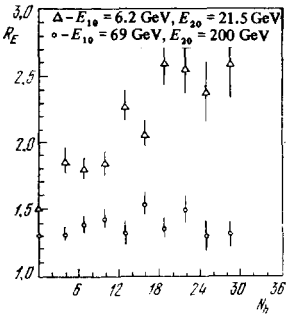

FIG. 11. The ratio $R_E = \langle n_s(N_h, E_{01})\rangle / \langle n_s(N_h, E_{02})\rangle$ as a function of the number N_h of highly ionizing particles in a star.[20]

Characteristic saturation properties can be detected in the behavior of n_s if we consider its correlation with N_h, n_g and compare data at different primary energies (see Sec. 2.9).

The multiplicity ratio for different primary energies E_0, i.e., $R_E = \langle n_s(N_h, E_{01})\rangle / \langle n_s(N_h, E_{02})\rangle$, plotted as a function of N_h (Fig. 11) shows some striking features. For primary energies below about 50 GeV, the ratio R_E depends on the number of highly ionizing particles in the star, N_h, but, at higher energies, this ratio remains constant and—this is particularly important—the value of the constant is close to the value of this ratio for elementary collisions (Table III). Thus, the mean multiplicity of shower particles ceases to "feel" the degree of excitation of the target nucleus at high energies. This property can be written in the form

$$\langle n_s(E_0,\ N_h)\rangle = \langle n_s(E_0)\rangle_H R_A(N_h),$$

where $\langle n_s\rangle_H$ is the mean multiplicity of charged shower particles in the hadron-proton interaction.

The ratio $R_A(N_h)$ also shows some interesting properties. Firstly, for the statistical data available at present, the results can be represented by the linear function $R_A(N_h) = a + bN_h$ (see Fig. 2b), where a is close to unity for primary energies in excess of about 100 GeV. Nuclear-emulsion data[7] obtained for protons of 200 GeV/c for events with $N_n \geq 2$, give $a = 1.11 \pm 0.04$. This value remains constant as the primary energy increases. Emulsion data on cosmic rays were analyzed in[21]. The mean energy of one group of events was about 11 TeV, whereas for another group it was $E_0 \approx 0.5$ TeV. The quantity R_A was estimated by using the ratio $R_A \equiv n_s/\varphi(E_0)$, where $\varphi(E_0)$ is the analytic expression for the multiplicity in pp interactions as a function of primary energy. The result of this analysis confirmed a conclusion that $a \approx 1$, and this was independent of primary energy (the slope b was also independent of energy). Moreover, this conclusion was practically insensitive to the method used to determine $\langle n_s\rangle_H$. It follows from Fig. 2b that R_A appears to saturate as a function of E_0 for any value of N_h. These limiting properties of the multiplicity ratios R_E and R_A are referred to as nuclear multiplicity scaling.[21,28] In particular, this result can be looked upon as a useful empirical rule that can be used to predict the multiplicity $\langle n_s\rangle$ for pA interactions from given pp data.

It is clear from the results summarized in Sec. 1.2 that the coefficients a and b depend on the angle of emission (pseudorapidity) of the secondary relativistic particle.

The Cracow group have reported[29] an interesting limiting property of the coefficients in the linear relationship between the multiplicities n_s and N_h for different ranges of values of the pseudorapidity $\eta = -\ln\tan(\theta_L/2)$. They used emulsion data for primary energies of 67, 200, and 3000 GeV (the experimental data were obtained in space). They found that, independently of primary energy, the region of development of the component b, which depends on nuclear excitation, is shifted relative to the region of development of the component a by two units of the pseudorapidity η. The conclusion must be that there is always a range $\Delta\eta$ of pseudorapidities which is independent of the target nucleus and of the primary energy. Along the λ axis, the size of this region is approximately equal to unity (see Sec. 1.2 where it was noted that the hadron-nucleus and hadron-nucleon distributions of pseudo-rapidities were identical). This fact remains unexplained. The weak dependence of quantities characterizing the degree of excitation or breakup of the target nucleus on n_b, n_g, and N_h is also exhibited by the variance D of the distribution of the multiplicity n_s of relativistic particles. Figure 4 shows the experimental dependence of $M = n_s/\sqrt{D}$ on n_g obtained in[25] for a group of interactions between protons and heavy nuclei in emulsions (Ag, Br). The primary energy was 200 GeV. It is clear that the dependence is very weak. This fact and the other properties of the distribution of n_s (for example, KNO scaling) indicate that the system of particles produced during the hadron-nucleus collision retains its properties for a period of time comparable with the time of propagation of the system in the nucleus.

1.4. Total cross sections for the interaction between hadrons and nuclei

It is now known that the experimental energy dependence of total cross sections for the interaction between hadrons and nuclei does not exhibit the simple asymptotic properties that were expected only a few years ago.

Here, we shall confine our attention to the two functions $\sigma_t(E_0)_{A=\text{const}}$ and $\sigma_t(A)_{E_0=\text{const}}$. There are good accelerator data on the energy dependence of the total cross section up to primary energies of about 300 GeV.

For protons, pions, and kaons of either sign, the cross section remains constant at primary energies of about 20–100 GeV in a broad range of values A[30]. The neutron-nucleus total cross sections at these values of

TABLE III. Nuclear interaction: p in nuclear emulsion[21]

E_{01}; E_{02}, GeV	R_E	R_{EH} (pp interaction)
21.5; 6.2	2.03±0.04	1.50±0.01
200; 69	1.31±0.03	1.30±0.03
300; 200	1.17	1.15

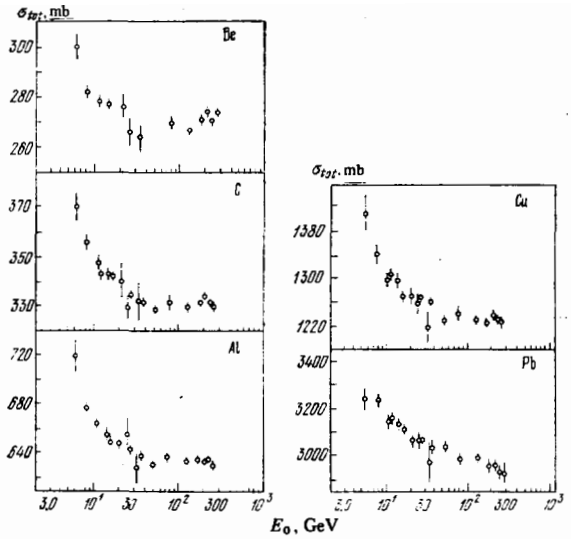

FIG. 12. Energy dependence of total neutron-nucleus cross section.[32]

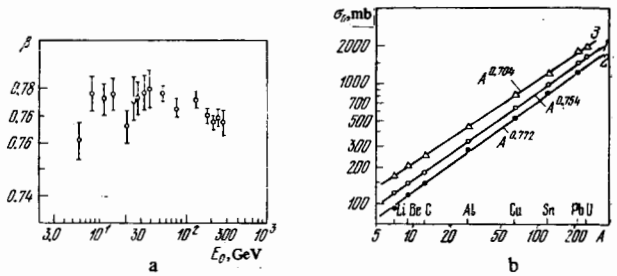

FIG. 13. a) Exponent β in the formula $\sigma_t = \sigma_0 A^\beta$ as a function of primary energy E_0 (σ_t is the total cross section for the interaction between neutrons and nuclei); b) absorption cross sections for positive pions (1), positive kaons (2), and protons (3) as functions of the mass number of the target nucleus at 30 GeV/c. Solid lines—power formulas.[30]

E_0 continue to fall with increasing energy.

The most detailed examination of the total cross section for the interaction between neutrons and nuclei up to primary energies of 270 GeV is given in[31,32]. Figure 12 shows the total cross section $\sigma_t(E_0)_{A=\text{const}}$, reported in[32]. It is clear from the figure that the well-known minimum in the nucleon-nucleon cross section near about 100 GeV is shifted even for the beryllium nuclei in the direction of higher energies. For the nC, nAl, and nCu cross sections, there is no observable increase with energy up to 270 GeV whereas, for nPb collisions, this cross section continues to decrease. The increase in the inelastic cross section for hadrons on light nuclei at primary energies $E_0 \gtrsim 200$ GeV has been found in a number of cosmic-ray experiments. There is an indication that the cross section continues to increase in the primary-energy region between about 1 and and 10 TeV. More detailed information can be found, for example, in[6].

For heavy nuclei, the above property of total cross sections does not appear to be valid. Thus, for example, the cross section for the interaction between hadrons and lead nuclei was investigated in[34]. The final result

TABLE IV.

E_0, GeV	Primary particles							Ref.
	π^+	π^-	K^-	p	$\bar{p}$	n	Hadrons	
20	$0.759\pm\pm0.008$	$0.738\pm\pm0.004$	$0.738\pm\pm0.007$	$0.691\pm\pm0.004$	$0.635\pm\pm0.010$			30
25		$0.742\pm\pm0.006$		$0.629\pm\pm0.009$				30
30	$0.751\pm\pm0.05$	$0.756\pm\pm0.005$	$0.761\pm\pm0.007$	$0.698\pm\pm0.004$	$0.651\pm\pm0.009$			30
40	$0.751\pm\pm0.008$	$0.754\pm\pm0.004$	$0.754\pm\pm0.006$	$0.691\pm\pm0.004$	$0.648\pm\pm0.010$			30
50	$0.726\pm\pm0.012$	$0.744\pm\pm0.004$		$0.697\pm\pm0.004$				30
60		$0.740\pm\pm0.004$		$0.691\pm\pm0.005$				30
30—300						$0.77\pm\pm0.01$		31
500							$0.72\pm\pm0.12$	11
600—4000							$0.71\pm\pm0.04$	34

agrees, to within experimental error, with the conclusion that the hadron-lead cross section is independent of energy. It would be premature to discuss these facts at present because the efficiency of systems used in cosmic-ray studies is a function of the energy and spatial parameters of secondary particles and of their multiplicity. This means that different fractions of the inelastic cross sections are recorded in different experiments.

Throughout the primary-energy band above 20 GeV, the measured total hadron-nucleus cross sections are found to be in agreement with a $A^{2/3}$ dependence, which indicates that there is a strong screening of the nucleons inside the nucleus (see Sec. 2.9). The nA cross section for $E_0 \gtrsim 30$ GeV was reported in[31] to be of the form $\sigma_t \sim A^{0.077\pm0.01}$. Table IV and Fig. 13a show the exponent β in the formula $\sigma_t = \sigma_0 A^\beta$ as a function of primary hadron energy. It is clear that β remains constant in a broad energy range, to within experimental error. The function $\sigma_t(A)$ is shown in Fig. 13b for different primary particles. The character of this dependence turns out to be dependent on the primary energy E_0. Thus, the authors of[14] studied the interaction between pions and C, Al, Cu, Ag, Pb, and U at the two primary-energy values $E_0 = 100$ and 175 GeV. They found that the absorption cross sections (like the cross sections at lower energies[31]) could be described by the single expression $\sigma_t \sim A^{0.75}$. The above experimental result is in good agreement with calculations based on the Glauber model, taking into account the energy dependence of the total hadron-nucleon cross sections.

1.5. Coefficient of inelasticity

The coefficient of inelasticity $\langle K \rangle$ is the fraction of primary energy transferred to secondary particles during an interaction. Existing experimental data suggest that $\langle K \rangle$ is approximately constant in a broad range of primary energies, at least up to $E_0 \approx 10$ TeV.

More detailed information can be found in[5,6]. Here, we shall briefly consider some of the properties of the coefficient of inelasticity specific for hadron-nucleus interactions.

TABLE V.

	Primary particle	Target			
		CH_2	Al	Fe	Pb
$\langle K_{\pi^0}\rangle$	All hadrons	0.22±0.01	0.24±0.01	0.25±0.02	0.26±0.01
$\langle K_{\pi^0}\rangle_3$	Charged hadrons	0.24±0.01	0.26±0.01	0.27±0.02	0.28±0.02
$\langle K_{\pi^0}\rangle_n$	Neutrals	0.17±0.01	0.19±0.02	0.19±0.02	0.21±0.02
$\langle K_{\pi^0}\rangle_\pi$	π^- Pions	0.33±0.02	0.38±0.04	0.37±0.05	0.39±0.04

TABLE VI.

Target	E_0, GeV	$\langle K_{\pi^0}\rangle$	Target	E_0, GeV	$\langle K_{\pi^0}\rangle$
LiH	100—500 100—300	0.15±0.04 0.19±0.03	Pb + Cu	300—600 600—1400	0.17±0.02 0.16±0.03

TABLE VII.

A	$\langle K\rangle$
C^{12}	0.65±0.08
Fe^{50}	0.76±0.09
Pb^{208}	0.92±0.11

To begin with, we note that $\langle K\rangle$ is not very dependent on the mass number of the target nucleus. This was investigated in detail using the cosmic ray flux at the Kum-Bel' high-altitude station of the Uzbek Physicotechnical Institute.[36] This installation could be used to determine the partial coefficient of inelasticity, i.e., the fraction of primary energy expended in producing neutral pions. The mean primary energy was about 400 GeV. The results are summarized in Table V for a number of values of A. The uncertainties indicated in this table are purely statistical. As can be seen, $\langle K_{\pi^0}\rangle$ is only slightly dependent on A. This is shown more clearly in Figs. 14a and 14b, where experimental results are compared with calculations based on the successive-collisions model (see Chap. 2). Calculations yield $\langle K_{\pi^0}\rangle \sim A^{0.12}$, whereas the experimental dependence for primary neutrons is $\langle K_{\pi^0}\rangle \sim A^{0.06\pm0.036}$. Finally, for all primary hadrons, $\langle K_{\pi^0}\rangle \sim A^{0.05\pm0.02}$ (see also[5,6]).

The conclusion that the coefficient of inelasticity $\langle K_{\pi^0}\rangle$ is only slightly dependent on A can also be deduced from the results reported in[37,38]. An ionization calorimeter was used in[37] to determine the partial coefficients of inelasticity $\langle K_{\pi^0}\rangle$ for $(CH_2)_2$ and lead. The mean energy of primary hadrons was about 400 GeV. It was found that $\langle K_{\pi^0}\rangle_{CH_2} = 0.18 \pm 0.04$ and $\langle K_{\pi^0}\rangle_{Pb} = 0.19 \pm 0.04$. The coefficient of inelasticity was investigated in[38] in the energy range 100 GeV $\lesssim E_0 \lesssim$ 1400 GeV. The results are summarized in Table VI.

The dependence of the resultant coefficient of inelasticity $\langle K\rangle$ on A for 200-GeV protons interacting with photoemulsion nuclei was analyzed in[25]. It was found that the coefficients of inelasticity for light (CNO) and heavy (Ag, Br) nuclei were the same to within experimental error: $\langle K\rangle_{CNO} = 0.53 \pm 0.03$, $\langle K\rangle_{AgBr} = 0.56 \pm 0.03$.

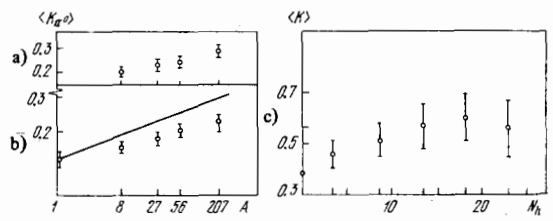

FIG. 14. Inelasticity $\langle K_{\pi^0}\rangle$ as a function of the mass number of the target nucleus (a, b).[36] a) All nuclear-active particles; b) primary neutrons (solid line—calculated from the successive collisions model; c) total inelasticity $\langle K\rangle$ as a function of N_h for collisions between protons and emulsion nuclei at initial energy $E_0 = 200$ GeV.[23]

The weak dependence of the resultant coefficient of inelasticity on A was also established for collisions between cosmic-ray nucleons and nuclei (primary energy $E_0 \approx 1350$ GeV[39]). This is shown in Table VII. The experimental data are described by the empirical formula $\langle K\rangle = (0.51 \pm 0.06)A^{0.09\pm0.03}$. This result was compared in[39] with Glauber-model calculations.[3)] The calculated result, i.e., $\langle K\rangle = 0.55A^{0.08}$, is close to that obtained by experiment.

The coefficient of inelasticity exhibits interesting properties as a function of the degree of excitation of the target nucleus. Existing experimental results indicate that $\langle K\rangle$ has only a very slight dependence on the state of the final nucleus. This conclusion follows, in particular, from Fig. 14c, which shows the experimental dependence of $\langle K\rangle$ on the number N_h of dense tracks in a star. These data were obtained by exposing nuclear emulsions to protons with momenta of 200 GeV/c.[23] The coefficient of inelasticity was determined from the angles of emission of secondary particles, using standard techniques of cosmic-ray physics, i.e., $\langle K\rangle = 1.5\langle p_\perp\rangle \sum(\cos\theta_i/E_0)$, where it was assumed that $\langle p_\perp\rangle = 0.35$ GeV/c. The secondary particle with the smallest angle of emission was excluded. It was found that, for $N_h \leq 7$ (for primary energies of 200 GeV, we have $\langle N_h\rangle \sim 7$), the coefficient of inelasticity $\langle K\rangle$ was a monotonically and slowly increasing function of N_h. It is clear that the leading particle carries off a major proportion of the energy. The coefficient of inelasticity remains practically constant ($K \sim 0.55$) as N_h increases further.

1.6. Transverse-momentum distribution of secondary hadrons

Detailed data on the values of $p_\perp$ in various types of collision are collected in[5,6]. We shall confine our attention here to the listing of the most reliably established experimental features of $p_\perp$, and will note new and important facts obtained in recent years. The established properties are as follows.

a) The mean transverse momentum of shower particles depends only very slightly on primary energy (see Secs. 2.6 and 2.9).

[3)] The Glauber model is briefly reviewed in the Appendix.

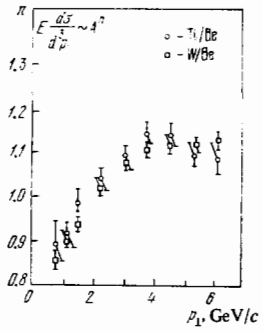

FIG. 15. Cross section for the production of pions with high transverse momenta $p_\perp$ as a function of the mass number of the target nucleus A.[40] Creation angle $\theta_{cms} = 90°$, $E_0 = 300$ GeV.

b) The distribution over $p_\perp$ in the case of secondary particles of a given type is sensitive to the nature of the primary particles. This property is a reflection of the conservation of the "leading" particle.

c) The dependence of $\langle p_\perp \rangle$ on the nature of the secondary particle has been reliably established. This quantity increases with increasing mass of the secondary particle (see Sec. 2.6).

d) The mean value $\langle p_\perp \rangle$ for shower particles from hadron-nucleus collisions is not very dependent on the degree of excitation of the target nucleus.

e) The transverse-momentum distributions are only very slightly dependent on primary energy in a broad range of values of E_0.

The observed mean transverse momentum of shower particles ($\langle p \rangle_s \sim 0.3$–$0.4$ GeV/c) is much smaller than the value predicted by the model based on the intranuclear cascade. The discrepancy is particularly sharp for energies $E_0 \gtrsim 100$ GeV, where the cascade model predicts that $p_\perp$ should increase with primary energy E_0, and the calculated data differ from experimental values by a factor of nearly two. This again confirms the fact mentioned above, namely, that the dissipation of primary energy in the nucleus is less intensive than one would expect from the successive-collision model.

Experimental results on the values of $p_\perp$ for primary energies $E_0 \gtrsim 1000$ GeV have been obtained as a result of studies of cosmic-ray interactions. These data are subject to considerable uncertainty but, nevertheless, they do suggest the following new properties of the transverse-momentum distribution:

1) The mean transverse momentum $\langle p_\perp \rangle$ for primary energies in the range 10^3–10^6 GeV increases slowly (possibly logarithmically) with energy.

2) The cross section for the production of particles with transverse momenta in excess of 2 GeV/c is already appreciable at $E_0 = 10^6$ GeV.

3) For primary energies between 10^5 and 10^6 GeV, both $\langle p_\perp \rangle$ and the cross section for the production of particles with high values of $p_\perp$ continue to increase.

Detailed analysis of hadronic interactions involving cosmic rays at energies in excess of 10^5 GeV is given in[41].

The transverse-momentum distribution at large values of $p_\perp$ exhibits a somewhat unexpected dependence on the type of target nucleus. The inclusive cross section for the production of particles with high transverse momenta at center-of-mass emission angles of 90° to the direction of the primary proton beam was investigated in[40] for Ti, Be, and W. The primary momentum was $p_0 = 300$ GeV/c. Figure 15 shows the dependence of the exponent n in the formula $Ed^3\sigma/dp^3 \sim A^n$ on the transverse momentum. Instead of the expected constant value $n \sim 2/3$ indicated by the total cross section as a function of A, experiment shows that n increases up to about 1.1 at $p_\perp \approx 3$ GeV/c.

1.7. Inelastic interactions of photons and leptons with nuclei

The interactions of photons and leptons with nuclei contain information on both the mechanism of the elementary event and, possibly, on the structure of intranuclear nucleons. It turns out that the sensitivity of measured quantities to different variants of the interaction model is sufficiently high. Thus, if we suppose that the cross section for the interaction between photons and an intranuclear nucleon is equal to the corresponding value in a free collision ($\sigma_{\gamma N} \sim 100$ μb), the mean free path of a photon in the nucleus, defined by $\lambda_\gamma = \sigma_{\gamma N}^{-1} \times (\text{density of nucleons in the nucleus})^{-1}$, turns out to be much greater than the nuclear diameter (~ 700 F $\gg 2R$). The photoabsorption cross section should then be proportional to the first power of the mass number A.

It is, in principle, possible that the dependence on A is weaker still. This possibility (see Sec. 2.8) is founded on the results of experiments on the photoproduction of vector mesons (ρ, ω, φ) on nucleons and nuclei, which show definite similarity bebtwen photons and hadrons. This similarity means that the mean free path of photons may turn out to be comparable with the nuclear size ($\lambda_\gamma \sim 3$F). The consequence of this will be that the primary flux in the nucleus will be reduced (screening of internal nucleons in the nucleus), and this should lead to $\sigma_{\gamma A} \sim A^{2/3}$ in the limit of very high energies.

The dependence of the total photoabsorption cross section on the mass number at given primary energy, and the variation of this dependence with energy, are important criteria for verifying theoretical models.

The most detailed study of the total photoabsorption cross section as a function of energy and mass number of the target nucleus is given in[41]. The primary-photon energy was varied between 4 and 18 GeV, and the targets were C, Cu, and Pb. The results reported in this paper are summarized in Table VIII. In this table, $\sigma_{\gamma A}$ is the total photoabsorption cross section and $A_{eff} = \sigma_{\gamma A}/\sigma_{\gamma N}$. The table shows that the effective mass number A_{eff} is independent to within experimental error of the primary energy, and the nucleon screening effect in the nucleus is smaller than the corresponding effect for hadrons. The absorption of photons by nuclei varies more slowly as a function of mass number than A, and we thus have an indication that there is a definite similarity between photons and hadrons although the experimental dependence on A is stronger than $A^{2/3}$. This is

TABLE VIII.

E_0, GeV	$\sigma_{\gamma C}$, μb	$\sigma_{\gamma Cu}$, μb	$\sigma_{\gamma Pb}$, μb	A_{eff}			A_{eff} : A, %		
				C	Cu	Pb	C	Cu	Pb
4.1±0.5	1305±52	5983±393	16680±1960	10.5±0.4	48.4±3.3	136.9±16.1	87.6±3.7	76.4±5.1	65.3±7.7
5.2±0.6	1288±38	5968±351	—	10.6±0.3	49.4±3.0	—	88.5±2.9	77.9±4.7	—
6.6±0.8	1278±34	5948±359	16760±1320	10.8±0.3	50.3±2.6	142.4±11.3	89.7±2.7	79.3±4.1	68.5±5.4
8.4±1.0	1238±32	5305±314	14930±1330	10.6±0.3	45.7±2.7	129.2±11.6	88.6±2.5	72.1±4.3	62.2±5.6
9.8±1.2	1219±62	—	—	10.6±0.5	—	—	88.2±4.5	—	—
10.7±1.3	1218±35	—	—	10.6±0.3	—	—	88.7±2.8	—	—
12.5±1.5	1161±31	—	—	10.3±0.3	—	—	85.4±2.5	—	—
13.6±1.6	1124±38	5380±353	12870±2200	10.0±0.3	47.9±3.2	115.0±19.7	83.1±3.1	75.5±5.0	55.3±9.5
16.4±2.0	1171±30	5228±352	15240±1860	10.5±0.3	47.0±3.2	137.5±16.9	87.5±2.6	74.1±5.0	66.1±8.1

confirmed by the data shown in Fig. 16, which gives the experimental function $A_{eff}(A)$.

Lepton-nucleus interactions can also yield indirect information on the photon-nucleus interaction. This is based on the assumption that the energy-momentum transfer is achieved in the reaction through a virtual photon.

Inelastic scattering of electrons by D, Be, Al, Cu, and Au was investigated in[42] for six values of primary electron energy in the range between 4.5 and 19.5 GeV. Reactions in which the electron energy loss $\nu_e = E_0 - E_h$ was between 2 and 14 GeV were recorded (ν_e is the virtual photon energy), and this corresponded to the energy region investigated in[41]. The nucleon screening effect was analyzed in the form $\sigma_{eA}/\sigma_{eN} = A_{eff} = A^{\delta}$, where σ_{eA}, σ_{eN} are, respectively, the inelastic electron scattering cross sections of the nucleus and the free nucleon, respectively. It was found that, throughout the range of values of ν_e, the exponent δ was equal to unity with a high degree of precision. The mean result for all the energies was $\langle\delta\rangle = 1.0003 \pm 0.0009$. The conclusion must, therefore, be that there is no screening effect. This is in clear contradiction to the results reported in[41]. However, the contradiction is removed if we recall that the experiments were concerned with different ranges of values of transferred 4-momentum q. In[41], $q^2 = 0$ for the real photon and, in[42], the energy range was $4(\text{GeV})^2 > |q^2| > 0.5(\text{GeV})^2$.

Inelastic scattering of electrons by nuclei at $|q^2| = 0.1$ $(\text{GeV})^2$ was investigated in[43]. The screening factor A_{eff}/A, obtained in this work for different values of virtural photon energy, is given in Table IX.

Comparison of Tables VIII and IX with the results

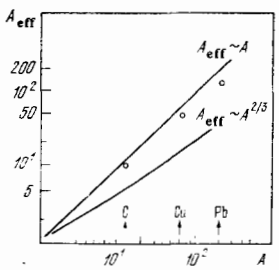

FIG. 16. Effective number A_{eff} of nucleons as a function of the mass number A in the case of photoabsorption in nuclei.[41] The data are averaged over primary energies in the range 3.7 GeV $\leq E_0 \leq$ 18.3 GeV.

TABLE IX.

ν_e, GeV	C	Al	Cu	Ta
2.00	0.896±0.024	0.919±0.026	0.865±0.024	0.872±0.030
2.87	0.960±0.027	0.888±0.028	0.937±0.033	0.900±0.034
3.91	0.928±0.028	0.909±0.026	0.882±0.030	0.870±0.033
4.90	0.914±0.034	0.915±0.037	0.933±0.043	0.900±0.043
8.45	0.961±0.040	0.925±0.044	0.815±0.042	0.859±0.045

in[42] leads to the conclusion that the screening effect is enhanced as the transferred 4-momentum q is reduced (for fixed ν_e). All the attempts undertaken so far to detect the anomalous muon interaction have yielded a negative result. This enables us to explain the nuclear interaction of muons within the framework of only photonuclear reactions. Unfortunately, there is very little experimental material in this field.

The interaction of 12-GeV/c positive muons was investigated on the Stanford linear accelerator, using an optical spectrometer based on a spark chamber.[44] The targets were C and Cu. The main conclusion of this work is that, for effective energies of the intermediate photon in the L system, which lead to an observed final state in the range $E_{0\gamma} < 3$ GeV [$E_{0\gamma} - \nu_\mu - (|q^2|/2m)$ and m is the nuclear mass], the reaction involves the participation of the entire volume of the nucleus. When $A_{eff} = \sigma_{\mu A}/\sigma_{\mu N}$, it is found that $\sigma_{\mu C}/\sigma_{\mu N} = 11.0 \pm 0.4$, $\sigma_{\mu Cu}/\sigma_{\mu N} = 63.1 \pm 2.2$, so that $\sigma_{\mu A} = \sigma_{\mu N} A^{0.99 \pm 0.01}$. The transferred momentum is in the range $0.2 \lesssim |q^2| \lesssim 0.3$ $(\text{GeV}/c)^2$. It is shown in[45] that the screening effect is determined by the simultaneous influence of the transferred four-momentum and the virtual energy of the photon, i.e., its mass. The data were obtained by measuring the inclusive scattering of positive muons with mean energy of 7.2 GeV on C, Al, Cu, Sn, and Pb. It was found that screening was absent for $x = q^2/2m\nu_\mu > 0.1$ (m is the nuclear mass). For $x < 0.1$, the experimental data indicate that $A_{eff} = A^{0.963 \pm 0.006}$.

Cosmic muons interacting with nuclei were investigated in a number of papers.[46,47] The experimental techniques were different, and the only common feature of this work is the method used to record and measure the energy of the nuclear showers. The cross section for the nuclear interaction of muons is deduced from experimental spectra through comparison with calculations, but there is always an arbitrariness in the choice of the parameter values that are introduced *a priori* into the calculations. The dependence of the muon photoabsorption cross section on the mass number A cannot be established in a pure form from these experimental results for a fixed effective energy $E_{0\gamma}$ of the intermediate photon because only one material was used in each experiment as the target. Moreover, different experiments cannot be compared either, because of considerable experimental uncertainties. Nevertheless, certain definite conclusions on the dependence of the interaction mechanism on A and on the energy $E_{0\gamma}$ can be established by reducing different experimental data to a common scale (Fig. 17). In actual fact, analysis of the experimental spectra yields the quantity $\sigma_{\gamma A} = \sigma_{\gamma N} A_{eff}^{exp}$, and the

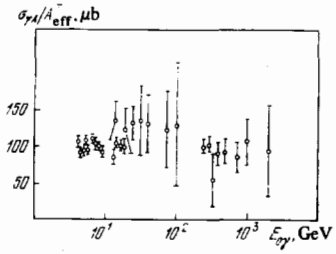

FIG. 17. Nuclear photoabsorption cross section $\sigma_{\gamma A}/A^{T}_{\text{eff}}$ ($A^{T}_{\text{eff}} = 0.22A + 0.78A^{0.89}$) as a function of energy.

TABLE X.

Process $\pi^- \to 3\pi$				Process $\pi^- \to 5\pi$, 15.1 GeV/c	
Mass range, GeV/c^2	σ, mb			Mass range, GeV/c^2	σ, mb
	15.1 GeV/c	13 GeV/c	8.9 GeV/c		
1.0—1.2	23±1.5	27±2	27±2	1.5—1.9	17±5
0.9—1.1	26±1.5	32±2	29±2		
1.1—1.3	20±1.5	22±2	23±2.5	1.5—1.7	10±7
1.3—1.5	17±2.0	15±3	5±2		
1.5—1.7	20±3.0	26±7		1.7—1.9	10±10
1.7—1.9	9±2.0	18±8			

energy dependence of this parameter reflects both the energy behavior of $\sigma_{\gamma N}$ and the shielding of nucleons in the nucleus. Figure 17 shows the experimental dependence of the quantity

$$\sigma_{\gamma A}/A^{T}_{\text{eff}} = \sigma_{\gamma N} A^{\text{exp}}_{\text{eff}}/A^{T}_{\text{eff}},$$

on the virtual photon energy, where $A^{T}_{\text{eff}} = 0.22A + 0.78A^{0.89}$. It is clear that, for primary energies $E_{0\gamma}$ between 10 and 1000 GeV, the interaction mechanism is essentially independent of energy. If we suppose that the cross section for the interaction with the intranuclear nucleon remains constant in this region, we must conclude that the screening of the nuclear volume does not increase with increasing energy.

1.8. Coherent and noncoherent production of hadrons on nuclei

Hadron-nucleus collisions with a fixed number of particles in the final state exhibits new and important features that are directly connected with the mechanism of multiple production and have forced a reconsideration of some of the theoretical ideas about this mechanism. The problems involved in the study of such interactions are quite complicated and varied. They have been reviewed in detail in a number of excellent publications.[48] It will be convenient to note here some of the main facts relating to the space-time development of the process in the nucleus (see Secs. 2.2–2.4).

The most complete investigation of the coherent process $\pi^- A - 3(5)\pi A$ was carried out on the proton synchrotron at CERN, using the spark chamber spectrometer.[49] A study was made of the reaction for primary-pion momenta of 9.9, 13, and 15.1 GeV/c, using Be, C, Al, Si, Ti, Cu, Ag, Ta, and Pb targets. The distributions over the 4-momentum transfer were obtained in these recent experiments with a very high precision and, as usual, contained two components, i.e., the coherent and the noncoherent reaction sums for the individual nuclear nucleons. The total cross sections for coherent production, obtained by subtracting the shallow noncoherent part from the differential distributions, increased with increasing mass number of the target nucleus, as expected from the optical model. The calculated total cross sections contained the total cross section for the interaction between the system of pions and the intranuclear nucleon as a parameter, and this was determined in[49] by fitting the coherent cross section to the experimental dependence on the mass number A. The final values for the different effective masses of the created system are listed in Table X. The errors indicated in this table represent only the statistical uncertainties.

The data in Table X lead to the following important conclusion: the cross section for the interaction between the system of pions and the nucleon does not exceed the cross section for an individual hadron (see also Secs. 2.2–2.4).

An analogous result was obtained in[50] as a result of a study of the coherent interaction between 11.7-GeV/c positive pions and nuclei. This work was carried out on the proton synchrotron at CERN, using the heavy-liquid bubble chamber filled with a mixture of propane and bromine containing freon. This meant that neutral pions could be directly detected. The Glauber approximation was used to extract the cross section for the interaction between the triplet $2\pi^+\pi^-$ and a nucleon, and it was found that, for effective masses of the triplet $2\pi^+\pi^-$ in the neighborhood of the mass of the A_1 meson, the cross section was $\sigma_{3\pi N} = 22^{+12}_{-7}$ mb.

The overall conclusion that the interaction inside the nucleus is small turns out to be independent of the quantum numbers of the primary particle. This is confirmed by the following examples, The coherent process $K^- A \to K^-\pi^+\pi^- A$ was investigated in[51] with a hydrogen-neon bubble chamber and a propane-freon chamber for negative kaon momenta of 5.5, 10.0, and 12.7 GeV/c and nuclei with $A \approx 20$. The cross section σ_{QN} for the interaction between the system $Q = K^-\pi^+\pi^-$ and an internal nucleon was determined by fitting the experimental total cross sections to the calculated values obtained in the Glauber approximation (σ_{QN} appears as a parameter). The zero-angle production cross section obtained in experiments with free protons was employed. For primary momenta of 10 GeV/c, this fit gave $\sigma_{QN} = 20.8^{+7.2}_{-9.0}$ mb for effective masses $M_{K\pi\pi} < 1.5$ GeV/c, and the result for primary momentum of 12.7 GeV/c was $\sigma_{QN} = 20^{+6.0}_{-8.4}$ mb. If we take the mean total cross sections for the $K^- p$ and $K^- n$ reactions, σ_{KN}, as a measure of the interaction with the free nucleon, experimental data show that $R = \sigma_{QN}/\sigma_{KN} = 0.98^{+0.24}_{-0.37}$. Thus, the cross section for the interaction between the system of particles and an intranuclear nucleon again does not exceed the cross section for a single hadron. In accordance with the quark model, one would expect $R \geq 2$ for uncorrelated K^* and π. The experiment reported in[52] was concerned with the transition $p - p\pi\pi$ on a neon target for primary-proton momenta of 28 GeV/c and it was found that $\sigma_{pN} \leq \sigma_{(p\pi\pi)N} \lesssim 1.8\sigma_{pN}$ to within experimental error.

There is experimental evidence that the suppression

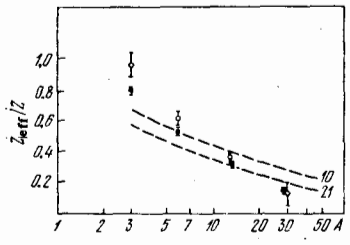

FIG. 18. Effective number Z_{eff} of protons for the reaction $\pi^- + A_Z \to \pi^0 + A_{Z-1}$ (1) and $\pi^- + A_Z \to \eta_0 + A_{Z-1}$ (2) for $E_0 = 48$ GeV.[53] The curves are calculated from the Glauber model for secondary-particle absorption cross sections of 10 mb (upper curve) and 21 mb.

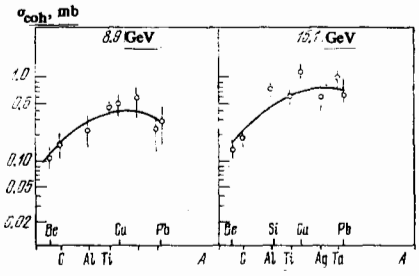

FIG. 20. Coherent production cross section for the system $2\pi^-\pi^+$ in the state $J^P = 0^-$ on nuclei. Primary pions with $E_0 = 8.9$ and 15.1 GeV.[49] Curves—calculated from optical model. For $E_0 = 8.9$ GeV, the absorption cross section is $\sigma_{3\pi N} = 60$ mb; $\sigma_{3\pi N} = 47$ mb for $E_0 = 15.1$ GeV.

of the interaction between hadronic systems inside the nucleus is not a property specific only for coherent processes. An example is provided by studies of inelastic charge-transfer processes between negative pions and π^0 and η^0 on nuclei for primary pion momenta of 48 GeV/c.[53] This work was carried out on the Serpukhov accelerator, using a spark chamber spectrometer incorporating lead plates (the $\pi^0 \to 2\gamma$ and $\eta^0 \to 2\gamma$ decays were investigated). The targets were Li, C, Al, and Cu. Reactions were isolated in which, in the final state, there were no additional charged particles with high energies or any other neutral particles apart from the recorded π^0 and η^0. The state of the target nucleus was not determined, but it was known that the amount of energy taken up by it was relatively small. The interaction of secondary particles in the interior of the nucleus can be described by the effective number of protons in the nucleus on which the charge-transfer process takes place, and this is defined by $Z_{eff} = \sigma_{\pi A}/\sigma_{\pi N}$. The cross section for the interaction of a secondary particle in the nucleus is present in Z_{eff} as a parameter. It was determined by fitting the experimental values of Z_{eff} to calculations based on the Glauber multiple-scattering model, using different assumptions about the density distribution in the nucleus. A comparison of the experimental data with the calculations is shown in Fig. 18. It is clear that, for the light nuclei Li and C, the experimental results are in agreement with the pion absorption cross section in the nucleus $\sigma_{\pi N} \sim 10$ mb. For heavy nuclei, the cross section $\sigma_{\pi N}$ turns out to be greater by a factor of two (~ 25 mb). Figure 19 shows the reaction cross sections as functions of the mass number of the target nucleus.

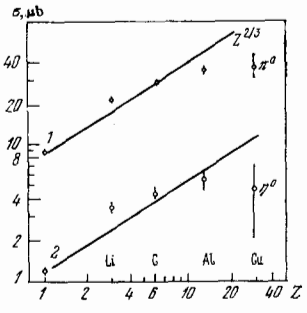

FIG. 19. Reaction cross section as a function of Z. The notation is the same as in Fig. 18.

Returning now to the results reported in[49], we note the observed dependence of the degree of absorption of the multipion system (3π) on its quantum numbers J^P. Phase-shift analysis can be used to isolate different spin and parity states, and this has shown that the cross section for the interaction of the 3π system in the $J^P = 0^-$ state with an internal nucleon exceeds the resultant cross section (Table X) by a factor of two or three. Figure 20 shows the cross section for the coherent production of the 3π system in the 0^- state as a function of the mass number A of the target nucleus for effective masses in the range $0.95 < M_{3\pi} < 1.25$ (GeV/c)^2. The figure also shows optical model calculations. The selected values of the 3π-nucleon interaction cross section were found to be $\sigma^{0^-}_{3\pi N} = 60 \pm 30$ mb at 8.9 GeV/c and $\sigma^{0^-}_{3\pi N} = 47 \pm 20$ mb at 15.1 GeV/c. The $J^P = 1^+$ state, which predominates at these energies, is absorbed to a much lesser extent: $\sigma^{1^+}_{3\pi N} = 23 \pm 1.5$ mb.

The above dependence of the absorption cross section on J^P is confirmed by data on coherent reactions at lower energies.[54] Estimates show that as the primary energy is reduced, the degree of absorption of the created system in the nucleus increases, and this can be explained by the increase in the relative contribution of states with lower spins and parities (including $J^P = 0^-$). In other words, as the energy is reduced, the properties of secondary particles inside the nucleus approach those in the free states.

Finally, we emphasize once again that we have not tried to achieve the impossible and provide a complete review of the experimental situation in the field of interactions with nuclei at high energies. The choice of the material was dictated largely by the possibilities of clear interpretation of experimental data and, to some extent, by personal tastes of the authors. It cannot, therefore, be regarded as reflecting the relative importance of the various topics. Several questions in relativistic nuclear physics that are undoubtedly of great importance for the future (including, above all, cumulative production of nuclei and the associated phenomenon of nuclear scaling[55,56]) have not been touched upon. In our view, they require a separate review.

2. MODELS OF THE INTERACTION BETWEEN HIGH-ENERGY PARTICLES AND NUCLEI

2.1. General remarks

At the present level of understanding of interactions occurring at high energies, it is convenient to establish, to begin with, at least a very rough classification of existing extreme points of view in relation to these phenomena.

One approach is to suppose that the interaction between hadrons and nuclei is either a one- or two-stage process.[57] The former view is adopted, for example, in the multiperipheral model, and the latter is used to describe the production and the subsequent decay of hadronic clusters. At the very least, this classification is not altogether satisfactory. Thus, the multiperipheral model and its parton treatment (see[2] and the discussion below) can hardly be regarded as involving a one-stage process: this model clearly separates the different stages of the interaction process, namely, the decay of the hadron into virtual (or real) groups of hadrons (partons), the interaction between slow particles in this group and the target hadron, and the production of secondary hadrons resulting from the collection or fragmentation of virtual particles (partons). Again, the cluster model can hardly be reduced to a two-stage process because the formation of the cluster and its subsequent decay develop in space-time, and the properties of the cluster may be substantially different at the different stages of its evolution.

Nor is it useful to separate processes into "instantaneous" and "extended" in space-time when we are dealing with the large number of particles (and, possibly, interactions) involved in collisions with nuclei.

In our view, the most reasonable approach at this stage of development of the theory is to classify existing ideas in accordance with the degree to which they take into account the collective character of the interaction with nuclei. The extreme points of view are then as follows: 1) all phenomena involving the interaction of particles with nuclei can be reduced to elementary interactions with quasifree nucleons and 2) the interaction with the nucleus cannot be subdivided even into two successive collisions, i.e., the primary collision results in the formation of a single hadronic system (cluster), the decay of which leads to the formation of the secondary particles.

The classical example of the first point of view is the simple model based on the intranuclear cascade (see, for example[6],). An equally classical example of the second point of view is the hydrodynamic model, in which the interaction process is regarded as being purely collective. We note that even this classification is not entirely satisfactory. Nevertheless, it appears to be more suitable than the others for the analysis of the complex phenomena which we have to face below.

Undoubtedly, the choice between the different theoretical alternatives is, in the first instance, dictated by agreement or otherwise with experimental data (see Chap. 1). Experiments indicate that many important characteristics of hadron-nucleus collision processes, such as the inelasticity coefficient K (see Sec. 1.5 and Fig. 14), the mean multiplicity $\langle n \rangle$ (see Sec. 1.1 and Fig. 3), the distribution of secondary hadrons over rapidities y (Sec. 1.2 and Fig. 6) and over transverse momenta $p_\perp$, and the abundance of secondary particles are slowly-varying functions of the number A of nucleons in the nucleus. The total cross section for the interaction between hadrons (real photons) and nuclei, on the other hand, is very dependent on A ($\sigma_{tot} \sim A^\alpha$, $\alpha \sim 2/3$) (see also Sec. 1.4 and Fig. 13). It is precisely these features of processes occurring on nuclei that must, in our view, be understood first.

Among the numerous theoretical models, we shall confine our attention to those that, in addition to explaining the main experimental facts (which is insufficient for an unambiguous choice of model) are the simplest and, at the same time, sufficiently general. The last criterion will ensure that the model will be able to explain, at least qualitatively, a broad range of phenomena (including the characteristics of elementary hadronic collisions) for a relatively small number of adjustable parameters. The most important of these are the hydrodynamic approach (collective interaction) and the parton version of the multiperipheral model (field-theoretical approach). At this junction, we encounter an important point: although the interaction of particles with nuclei is a single process, it can conveniently and usefully be divided into two phenomena which manifest themselves in the longitudinal (relative to the momentum of the incident particle, $\mathbf{p}_0$) and transverse[4)] directions. Processes occurring in the longitudinal direction appear to have essentially different physical meaning than those occurring in the transverse direction.

Since $\langle p_\perp \rangle$ is bounded, new particles will be produced in the longitudinal direction. In other words, the development and subsequent decay of virtual states that are responsible for the production of new particles take place in the longitudinal direction.

In the transverse direction, the momentum is transferred to the nucleus A and is distributed among its nucleons. The processes associated with this are determined largely by the properties of nuclear matter and its excitations. The development of the process in the longitudinal direction determines the properties of the system of n_s shower particles whilst, in the transverse direction, it determines the system of N_h highly ionizing particles.

Roughly speaking, processes developing in the longitudinal and transverse directions can be ascribed the characteristics shown in Table XI.

In general, the coupling between processes developing in the two directions is so weak that these processes can be discussed independently. This important point requires further elucidation. It is possible that the size of the virtual phase exceeds substantially the linear di-

[4)] We are concerned here with directions for which the angle of emission in the center-of-mass system is $\theta_{cms} \lesssim 1$.

TABLE XI.

Longitudinal motion	Transverse motion
New particles appear	New particles are practically not formed
Relativistic motion of matter	Motion of matter nonrelativistic
Motion almost one-dimensional at all stages	Motion isotropic during final stage
Ultrarelativistic equation of state	Equation of state corresponds to the nonrelativistic form of motion of nuclear matter

mensions of the nucleus at high energies (this is the case in the tube and parton models described below). Any correlation between the longitudinal and transverse parameters [for example, $n_s(N_h)$] will therefore be determined only by the magnitude of the momentum transferred to the nucleus during the virtual phase, and by the properties of nuclear matter. It is quite possible that here we have the key to the puzzle of the asymptotic property $N_h(E_0) = \text{const}$ (see Sec. 1.3). The mean momentum transferred to the nucleus in the transverse direction is independent of E_0! We shall be interested largely in "longitudinal" processes connected with mainstream high-energy physics. [5)]

2.2. Interaction between hadrons in nuclear matter and coherent production of hadrons on nuclei

Consider the following hadron production processes in hadron (photon)-nucleus collisions:

$$a + A \to b + A, \quad (1)$$
$$a + A \to c + A', \quad (2)$$

where a is the incident hadron (photon), b is the secondary hadron or a system of secondary hadrons with internal quantum numbers identical to the quantum numbers of the incident particle a, possibly with the exception of spin and parity, A is the target nucleus, c is a hadron or a system of hadrons with arbitrary quantum numbers, and A′ is the residual nucleus, nuclear fragments, and nuclear excitation products.

Process (1), in which the nucleus does not change its state, is called a coherent production process. It is due to the exchange of states with vacuum quantum numbers (vacuum reggeon or pomeron P) or ω-meson quantum numbers (ω-reggeon). The quantum numbers of the resulting system b then satisfy the semiempirical Gribov-Morrison selection rule, [58,59]

$$P_a = P_b(-1)^{\Delta S_{ab}}, \quad (3)$$

where P_a and P_b are the internal parities of the hadron a and the system b, and $\Delta S_{ab} = S_a - S_b$ is the difference between the total spins of a and b.

The charge, isospin, and strangeness of the system b are the same as for the particle a. The G and C parities do not change in the course of pomeron exchange, but change sign on ω-reggeon exchange. Only coherent production processes due to pomeron exchange take place at high energies. The cross sections for processes involving ω-reggeon exchange fall off as E_a^{-1}, where E_a is the energy of the particle a in the laboratory system (L system). Processes such as (2), which involve a change in the state of the nucleus A as a result of the interaction, are called noncoherent production processes. Here, we have, at least in principle, the possibility of exchange of any quantum numbers and the creation of the states c with arbitrary internal quantum numbers.

The theoretical description of coherent and noncoherent production of hadrons on nuclei is based on the Glauber method[60] (see, also[61,64],). Comparison of experimental data, obtained during the last few years, with the theoretical prediction has led to a number of very important qualitative and quantitative results with regard to the behavior of hadrons and hadronic systems inside nuclear matter (see Sec. 1.8). Our main aim here is to discuss, from the theoretical point of view, some of the experimental information in this area (see Sec. 1.8).

We recall that the Glauber method can be applied to the square of 4-momentum transfer t to the nucleus and the effective mass m_b of the hadronic jet b (or c) in order to determine the connection between the differential cross sections for processes (1) and (2), $d\sigma_A/dt\,dm_b$, and the differential cross sections $d\sigma/dt\,dm_b$ of the processes

$$a + N \to b + N, \quad (4)$$
$$a + N \to c + N, \quad (5)$$

on free nucleons. If we know the parameters of processes (4) and (5), we can calculate $d\sigma_A/dt\,dm_b$ for processes taking place on nuclei. The approximate results obtained in this way are as follows:

For coherent production ($t' \lesssim R^{-2}$)

$$\frac{d^2\sigma_A}{dt'\,dm_b} = \frac{d^2\sigma_N}{dt'\,dm_b}\Big|_{t'=0} N^2_{\text{coh}}(A, \sigma_{aN}, \sigma_{bN}, t'). \quad (6)$$

For noncoherent production ($t' \gg R^{-2}$)

$$\frac{d^2\sigma_A}{dt'\,dm_b} = \frac{d^2\sigma_N}{dt'\,dm_b} N_{\text{noncoh}}(A, \sigma_{AN}, \sigma_{cN}), \quad (7)$$

where $t = -q^2 > 0$, $t' = t - t_{\min}$, $t_{\min}$ is the minimum value allowed by the conservation laws governing the square of the 4-momentum transfer between particle a and the system b, $t_{\min} \approx (m_b^2 - m_a^2)/4p_a^2$ for $p_a \gg m_a$, m_b, p_a is the momentum of the particle a in the L system, $R = r_0 A^{1/3}$ is the nuclear radius, and $r_0 \approx 1.1$ F is the size of the nucleon. The quantities N_{coh} and N_{noncoh} are the effective numbers of nucleons participating in coherent and noncoherent production. [6)] These quantities can be measured through direct comparison of data for nuclei with

[5)] We come across here the profound question of the connection between high-energy physics and nuclear physics.

[6)] A simple derivation of the formulas for N_{coh} and N_{noncoh} in the optical approximation is given in the Appendix and in[51].

data for free nucleons.[7] Calculations based on the Glauber method show that the effective number of nucleons in a nucleus depends on the cross section σ_{aN} for the interaction between the primary particle a and the nucleon, and the cross section for the interaction between the secondary hadrons from the system $b(c)$ and nucleons. We have used σ_{bN} and σ_{cN} to denote the cross sections for the interaction of all the j hadrons from system $b(c)$ with nucleons in the nucleus: $\sigma_{bN}=\{\sigma_{b_1N};\ldots;\sigma_{b_jN}\}$, and similarly for σ_{cN}. The appearance of the dependence on σ_{aN}, σ_{bN}, and σ_{cN} in (6) and (7) has a simple physical interpretation: the Glauber method takes into account the absorption of the incident and emergent hadronic waves in nuclear matter (see Appendix).

Analysis of experimental data based on the Glauber method can be used to obtain important and interesting information on hadron-nucleon cross sections in an extended nuclear medium. In particular, this method has been used to determine the cross section for the interaction between the unstable hadronic resonances ρ, ω, φ, f, η^0, K^*, on the one hand, and nucleons, on the other (see Sec. 1.8). This information cannot be obtained in any other way. Henceforth, we shall be interested in multiparticle processes of the form

$$\pi + A \to 3\pi(5\pi,\ 7\pi, \text{etc.}) + A, \tag{8}$$

$$K + A \to 2\pi K\ (3\pi K,\ \text{etc.}) + A, \tag{9}$$

$$p + A \to \pi N\ (2\pi N,\ \text{etc.}) + A, \tag{10}$$

and so on.

Studies of processes of this kind have led to unexpected and interesting results (see Sec. 1.8).

2.3. States of hadrons created in the nucleus

It would appear at first sight that if a collision between an incident particle a and a nucleon in the nuclear interior results in the creation of a number of hadrons inside the nucleus, then during their subsequent motion inside the nucleus the secondary hadrons would interact with the internal nucleons independently of one another. For example, if three pions are created, then by comparing experimental data with theoretical formulas such as (6), it should be possible to establish whether the absorption of secondary pions in the nucleus results in a reduction in their number leaving the nucleus. Since, in this approach, the pions are assumed to interact independently of one another, the observed cross section for the absorption of the 3π system in the nucleus should be equal to three times the cross section for the inelastic πN interaction, i.e., $\sigma_{3\pi N}\approx 3\sigma_{\pi N}$. Similar considerations applied to a system of five pions should yield the result $\sigma_{5\pi N}\approx 5\sigma_{\pi N}$.

However, experimental data (see Sec. 1.8) show that these predictions are incorrect. Experiment shows that $\sigma_{3\pi N}\approx\sigma_{\pi N}$, $\sigma_{5\pi N}\approx\sigma_{\pi N}/2$, and $\sigma_{2\pi KN}\sim\sigma_{KN}$. This unexpected result requires careful analysis of the physical meaning of the observed phenomenon. The observed effect shows that hadrons in nuclear matter (at least, at distances of the order of the nuclear radius R) behave quite differently as compared with the rare collisions with protons in the hydrogen bubble chamber, where the mean distance between the protons is $\sim 10^{-8}$ cm.

One gains the impression that, for some very basic reasons, the cross section for hadron-nucleon interactions in the nuclear interior is smaller than the cross section for "the same" collision in vacuum. There is another approach to this apparently paradoxical situation: we could suppose that hadrons created in the nuclear interior form a single hadronic system (condensation or cluster) for some intermediate period of time (of the order of the time taken to transverse the nucleus), which is similar to an individual hadron or a quasistable (due to time dilation) resonance in the sense that it interacts with nucleons inside the nucleus as one whole with a cross section of the order of, or even less than, the ordinary hadron-hadron interaction cross section.

However, there is an essential difference between a resonance and a cluster: the latter does not have fixed quantum numbers. It is also important to emphasize that, so far, there is no unified definition of a cluster and this inhibits the understanding of models based on the cluster assumption. (The uncertainty in the concept of clusterization is discussed, for example, in the review paper[65] and the monograph[2].) It is possible that the two solutions (reduction in interaction cross section and formation of clusters) are not mutually exclusive ideas. Since we have no other alternative "languages" at our disposal, we shall consider both approaches to the solution of the problem.

2.4. Regeneration of hadronic states[8]

A classical example from electrodynamics was quoted in[66]. This involved the process of bremsstrahlung from a fast electron during large-angle scattering for which it is possible to investigate rigorously the change in the structure of the electromagnetic field of the electron throughout the entire interaction time. It was shown that, for a certain period of time, called the regeneration time, the electron that had instantaneously changed the direction of its motion behaved as if it were partially "stripped" or "semibare." This graphic terminology is meant to suggest that virtual photons are absent for a certain definite period of time from the electromagnetic field of the scattered electron within a certain frequency band. A finite time is necessary to ensure that the field of the electron is reestablished to its normal level and the electron is capable of emitting photons in this frequency band in the new direction of motion. The essence of this effect is that the rearrangement of the field of the scattered electron cannot take place instantaneously. There is no field in the direction transverse with respect to the new electron momentum $\mathbf{p}$ at a distance $r_\perp \gtrsim k^{-1}\gtrsim m_e^{-1}$ for a time $\tau_{reg}\sim p/m_e k_\perp$ (m_e is the electron

[7] The neutron cross sections are obtained from experimental data for deuterium targets.

[8] In this section we follow[66,67].

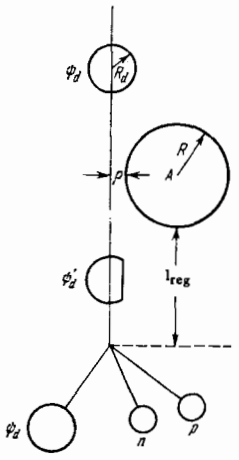

FIG. 21. Illustrating the differential generation of a deuteron with wave function ψ_d on a nucleus A. Impact parameter $\rho < R_d$—radius of deuteron; ψ'_d—"truncated" wave function for the deuteron after scattering; l_{reg}—regeneration length.

mass, $k_\perp$ is the transverse momentum of the bremsstrahlung photon emitted into a cone around the direction of **p**). If the time elapsed after scattering is $t \lesssim \tau_{reg}$, the field due to the electron and the field of the bremsstrahlung radiation along **p** are not separated in space and interfere destructively in a certain frequency band. It is only for $t \gtrsim \tau_{reg}$ that this nonequilibrium system decays into the bremsstrahlung photon and the "normally clad" electron. It is clear that, for $t \lesssim \tau_{reg}$, the semibare elec tron cannot emit bremsstrahlung photons in a certain range of momenta even if it again undergoes scattering within this period of time. Such bremsstrahlung photons can be emitted only after time $t \gtrsim \tau_{reg}$.

The above effect is observable and plays an important role in multiple electron scattering in a medium at high energies, in transition radiation, and so on.[66]

This example enables us to understand, at least qualitatively, the process that might be involved in the case of hadrons created in the interior of a nucleus. The observed reduction in the hadron cross section inside the nucleus may be due to similar reasons, i.e., the finite time necessary for the reestablishment of the mesonic field of hadrons. For a certain period of time, the hadrons produced inside the nucleus turn out to be "bare" or "semibare," so that their interaction with internal nucleons is much weaker than between hadrons clad by the normal field.

However, qualitative analysis of hadron-nuclear interactions is complicated by the absence of a rigorous theory capable of describing the development of the interaction process in time. One must therefore turn to models and qualitative analogies. Thus, the authors of[66,67] have given an example that can be used to follow the phenomenon of regeneration of hadronic fields during the interaction of hadronic systems. They have considered the diffractional dissociation of the deuteron on a perfectly absorbing nucleus with a sharp edge. Figure 21 illustrates the collision of a deuteron d with a nucleus A.[66,67] Suppose that the deutron approaches at a distance $\rho < R_d$ from the edge of the nucleus (R_d is the deuteron radius), and that it is known that the nucleus remains unexcited. It is clear that the necessary condition for this is that the neutron and proton in the deuteron must approach one another quite closely. Consequently, the wave function for the final state of the deuteron, ψ'_d, differs from the normal wave function ψ_d by the fact that the probability of finding the proton and neutron at a short distance $r < R_d$ from one another in the final state is greater than in the initial state. The final state is thus a nonequilibrium situation and can be represented as a superposition of the normal state of the deuteron with states corresponding to the free motion of the proton and deuteron ψ_f:

$$\psi'_d = C_0\psi_d + \sum_f C_f\psi_f,$$
$$|C_0|^2 + \sum_f |C_f|^2 = 1. \qquad (11)$$

However, these wave functions are not separated in space at the initial time: the nucleons can separate in the transverse direction to a distance $r > R_d$ not earlier than the time $t \gtrsim R_d/v$, where v is the relative velocity of the nucleons in the deutrons ($v \sim 0.15$ sec). In the laboratory system, the "truncated" deuteron with wave function ψ'_d will traverse during this time a distance $l \sim E_d R_d/m_d v$, where E_d is the initial deuteron energy and m_d is the deuteron mass. If the next nucleus is at a distance $r \lesssim l$ from the first, one would expect that the interaction cross section of the "truncated" deuteron and the nucleus would not be greater, and most likely be smaller, than the normal cross section.

Let us now consider the diffractional dissociation of a nucleon (10), assuming that the "normal" hadron size is $\sim \mu^{-1}$, where μ is the pion mass. After collision with the nucleus, the wave function ψ'_N for the state which describes the secondary excited nucleon has an analogous form to that given by (11):

$$\psi'_N = C_0\psi_N + \sum_{N^*} C_{N^*}\psi_{N^*} + \sum_{\pi N} C_{\pi N}\psi_{\pi N} + \sum_{\bar{K}KN} C_{\bar{K}KN}\psi_{\bar{K}KN} + \ldots, \qquad (12)$$

where ψ_N, ψ_{N^*}, $\psi_{\pi N}$, and $\psi_{\bar{K}KN}$ are the wave functions for the normal states of the nucleon, the isobars, the systems $\pi + N$, $\bar{K} + K + N$, and so on. The coefficients C_i determine the decay probabilities for the state ψ'_N into the corresponding hadronic states. These hadronic states can separate out in space in the transverse direction to distances $\rho \sim \mu^{-1}$ only after a time $\tau_{reg} \sim E_a/\mu m_b$, where m_b is the mass of the resulting hadronic system. This means that, during the time $t < \tau_{reg}$ after the collision, the size of the hadronic system and, consequently, its cross section for the interaction with internal nucleons may turn out to be smaller than for the initial hadron a. One further far-reaching hypothesis was put forward in[67], namely, it was suggested that the formation of the hadronic system with a large mass was accompanied by a considerable deformation of the field of the initial particle. If this hypothesis is correct, the subsequent interaction of the heavier hadronic condensations with internal nucleons must be characterized by a smaller cross section than for light condensations.

Let us estimate the regeneration time for the case where the effective mass of the 3π system formed by coherent production is $m_{3\pi} \sim 2$ (GeV/c)^2 for an initial pion

energy of 15 GeV. This is given by $\tau_{reg} \sim 7.5\ \mu^{-1}$.[9] This means that, for the 3π system, the free path associated with the interaction with internal nucleons will exceed the normal free path by a factor of three [the range in the nucleus of a hadron h for which $\sigma_{hN} \sim 20$ mb is $l_h \sim (\rho_A \sigma_{hN})^{-1} \sim 2\ \mu^{-1}$].

During the motion of the hadronic condensation inside the nucleus, the cross section for its interaction should increase due to the formation and decay of normal hadrons into which the initial condensation decays.

It will be interesting to analyze existing and future experimental data with allowance for the space-time development of hadronic systems formed during collisions between hadrons and intranuclear nucleons, especially in heavy nuclei. This can be based on the following formula put forward in[67,68]:

$$\sigma_{bN} = \sigma_0 e^{-vz/v\tau_{reg}} + \sigma_1 (1 - e^{-z/v\tau_{reg}}), \qquad (13)$$

where z is the distance traversed by system b inside the nucleus, σ_0 is the bN interaction cross section at the time of formation of system b, σ_1 is the bN interaction cross section for $z \to \infty$ when system b has decayed to normal hadrons, and v is the velocity of system b, whose magnitude is given by $v = \sqrt{1 - (m_b/E_b)^2}$.

It is expected that $\sigma_1 \sim \sum_i \sigma_{iN}$, where σ_{iN} is the cross section for the interaction between a hadron in system b and a free nucleon.[67,68]

The foregoing account enables us to put forward the following very probable hypothesis: for a certain period of time, comparable with that taken by a particle to traverse the nucleus, the particle partially "loses" its field. The field quanta and the remaining "semibare" particle subsequently interact with the nucleus independently of each other. In the first approximation, we can consider the superposition of the primary particle traversing the nucleus and "all the other" accompaniments. These ideas have been used as the foundation for a number of empirical models.[27,68]

In addition to diffractional production processes, there are also other facts supporting the idea that the states of hadrons inside a nucleus are modified as compared with states in a vacuum. In particular, it has long been known that, during an interaction with a nucleus, the mean inelasticity $K(A)$ for a leading particle (nucleon) is a slowly-varying function of A (see Sec. 1.5 and Fig. 14). This has led to the proposal that the cross section for the interaction between the primary nucleon and an intranuclear nucleon is reduced after the first collision in the nuclear interior.[69]

The model put forward in[68] is based on two fundamental assumptions: 1) the interaction between the leading particle and nucleons in the nucleus is independent of the states of the remaining secondary particles and 2) the nucleus is looked upon as a structureless liquid, the properties of which are such that the free path λ_1 of the leading particle up to the first interaction, and the free path up to the second interaction, are related by the inequality $\lambda_2 > \lambda_1$.

This model is essentially based on the above-mentioned possibility of separating the motions of the primary particle and "all the rest." Here, we investigate the motion of the primary particle in the nucleus in the language of free paths (or cross sections). Comparison with experimental data on leading particles then shows that their free paths inside the nucleus are substantially greater (by factors of 3–5) than one would expect on the basis of measured cross sections for the interactions between hadrons and free nucleons.

A further and more complicated phenomenological model has also been put forward.[27] In this approach, the first interaction event is accompanied by the appearance of a leading hadron and a certain hadronic cluster which subsequently interacts with the internal nucleons quite independently. The initial size of this cluster is assumed to be μ^{-1} and the cluster subsequently expands isotropically with velocity approaching the velocity of light. When the density falls to the critical value $\sim \mu^4$, the cluster begins to decay. The cross section for the interaction between the cluster and the nucleons is assumed to be substantially smaller than the hadron-nucleon cross section. We shall not be able to discuss all the details of this complicated model here and will merely note that some of the postulates upon which the model is based[27] are in the spirit of the statistical theory with an expanding volume[70] and the hydrodynamic theory (see below). The model is successful in explaining a number of experimental results (for example, see Fig. 8). It is not clear, however, whether the secret of its success is that it incorporates a large number of adjustable parameters.

2.5. Internal cascade model

It is clear from the foregoing that the simple variant of the cascade model, based on the hypothesis of successive and independent collisions between primary and secondary particles with intranuclear nucleons, with interaction cross sections equal to those in the case of quasi-free nucleons, is, at the very least, too naive and must be abandoned. Doubts about the validity of the model were expressed as far back as 1954[71] because the weak dependence of the multiplicity of secondary particles on A could not be understood within the framework of this model. The model is also in conflict with the weak dependence of other parameters on A, namely, the inelasticity $K(A)$, $\langle p_\perp \rangle$, and so on (see Chap. 1 and, especially, Fig. 14). To "save" the internal cascade model, one must introduce the following two *ad hoc* assumptions.

a) The cross sections for the interaction between secondary hadrons and intranuclear nucleons is substantially smaller than the corresponding cross section for free nucleons.

b) Cascade processes involve only a small fraction of secondary particles produced in the first interaction event. The remaining particles interact collectively.

[9] Experimental data on the behavior of this system inside the nucleus are discussed in Sec. 1.8.

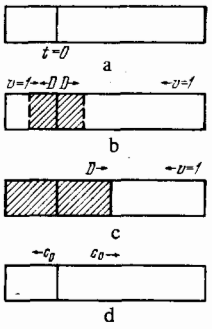

FIG. 22. Hadron-nucleus interaction in the hydrodynamic interpretation: a—initial instant of collision of hadron with tube of nuclear matter; b—propagation of shock waves in the hadronic fluid; c—end of shock-wave propagation and beginning of outflow of hadronic fluid into vacuum, d—simple rarefaction wave propagates through nuclear matter.

The first assumption is equivalent to the assumption of a local reduction in the density of nucleons in the nucleus as the hadronic shower traverses the latter.[72,73]

Monte Carlo calculations for this case can be used to obtain agreement with experiment up to primary-proton energies of $E_p \lesssim 70$ GeV.[72,73]

The second assumption is similar to the model involving a leading particle and a cluster showing a weak interaction with nuclear matter,[27] which was discussed above. In the first approximation, this assumption leads to an incorrect dependence of multiplicity on A, namely, $\langle n(A)\rangle \sim A^{1/3}$.

More detailed calculations[74] lead to a still stronger dependence. Of course, the cascade model parameters can always be adjusted to achieve agreement within some restricted energy interval, so that experimental results can be described. It is, however, still totally unclear which particular assumptions and how many parameters will have to be introduced into the theory in order to describe the experimental data, if only qualitatively, throughout the range of energies that has been examined so far.[10)]

However, the more fundamental point is quite different: the two assumptions that are necessary to "correct" the cascade model are essentially equivalent to the introduction of an extended virtual phase. It is therefore better, from the physical point of view, to treat the virtual phase in space-time directly.

2.6. Interpretation of the interaction of hadrons with nuclei

Without going into the history of the problem, and leaving to one side the mathematical formalism of the hydrodynamic theory of multiple production,[76,77] we recall its basic assumptions in relation to the hadron-nucleus collision:[71]

1) It is assumed that the interaction of the incident hadron takes place collectively with the nucleons lying along the path of the hadron in the nuclear material. The primary hadron, in effect, cuts out a cylindrical tube of radius of the order of μ^{-1} inside the nucleus (μ^{-1} is the effective size of the interaction region in the transverse direction) and height equal to the longitudinal size of the nucleus in the reference frame in which the collision between the hadron and the tube takes place.

2) The tube of hadronic material is assumed to be structureless and, in this sense, can be regarded as an individual particle of mass equal to the total mass of nucleons in the tube.

3) At the initial time of the collision process, the hadron and the tube are compressed disks, in accordance with the Lorentz contraction of longitudinal dimensions in reference frames moving relative to the laboratory frame.

4) The collision between the hadron and the tube is analyzed in the system in which the velocities of the hadron and of the tube are in opposite directions and are equal in absolute magnitude (equal-velocity frame).

5) The two disks come into contact at the initial time (Fig. 22a) and, thereafter, shock waves begin to propagate through the hadronic fluid with speeds D in both directions away from the contact plane. The material between the waves remains at rest (shaded part of Fig. 22b). After a certain time $t \approx r_0/D\gamma$ ($r_0 \sim \mu^{-1}$ is the size of the hadron in the rest system and γ is the Lorentz factor), the shock wave reaches the "boundary" of the hadron (Fig. 22c). The flow of the hadronic material from the left-hand part of the system into the vacuum begins at this time, and a simple rarefaction wave runs through the nuclear medium (Fig. 22d) with the velocity of sound c_0. When $c_0 > D$, and the number of nucleons in the tube is $n_{\text{tube}} > 4$, the simple wave will catch up with the shock wave and, after reflection from it, will give rise to the first reflected wave. The shock wave moving to the right eventually reaches the edge of the tube and this instant marks the beginning of the outflow of the material into vacuum whilst a rarefaction wave is sent out to the left. The hydrodynamic outflow continues until the density of the hadronic material falls to $\sim \mu^4$, i.e., the characteristic density of hadronic matter. At this time, the hadronic material begins to decay into real hadrons, in accordance with the laws of statistics or thermodynamics, provided the number of secondary particles is large.

We emphasize that assumptions 1)–5) do not form a set of independent postulates of the hydrodynamic model. Apart from the hypothesis involving the collision with a tube of nuclear matter, these assumptions are a consequence of two fundamental hypotheses, namely, the formation of the Lorentz-contracted volume in which the "classical" fluid is at rest, and the establishment of a local statistical equilibrium over the entire extent of the hydrodynamic outflow. We note that, during the initial stages of the hydrodynamic outflow, quantum corrections may possibly play a role in this process. A discussion of this point can be found in[77].

Essentially, if we use the modern jargon, the hydrodynamic model corresponds to the one-dimensional separation of two clusters moving in opposite directions

[10)] A similar discussion of the cascade model and of the results of numerical calculations corresponding to its various modifications are given in the monograph[6] and the review paper[75].

(see, for example,[78]). The interrelation between the clusters appears through the conservation laws. It is important, however, to emphasize that the formation, separation, and decay of clusters are described within the framework of this model on the basis of relatively general postulates.

In the specific solution of hydrodynamic equations, it may be necessary to take into account dissipative processes (viscosity), but we have neglected these processes for simplicity (this question is discussed in[77]).

We now note two further points. Qualitative analysis[79] shows that, in the hydrodynamic model, the leading nucleons should not enter the compound system if they obey the laws of relativistic hydrodynamics. Because of the operation of Pauli's principle, the nucleons should be ejected to the periphery of the hadronic material.[79] These ideas are so qualitative they are best regarded as additional postulates of the theory and this, unfortunately, is the weak point of the model. Thus, in hydrodynamic models, the entire hadronic system automatically decays into two hadronic clusters, which obey the laws of hydrodynamics, and leading particles. The characteristics of a leading particle are the adjustable parameters of the theory. The hydrodynamic model thus presupposes the separation of the interaction process into three main stages, namely; 1) the initial formation of a condensation of hadronic matter in some initial volume; 2) hydrodynamic outflow of hadronic material; and 3) decay of hadronic material into real hadrons.

But there is still one further important point. The characteristic ranges of the elements of the fluid prior to their decay are substantially greater than the Lorentz-contracted nuclear dimensions. Thus, for slow particles, this distance is $\sim r_0$ whereas, for fast particles, it becomes $\sim r_0\sqrt{E_0/M}$ (see[2]). Thus, the system largely decays into real particles outside the nucleus. The characteristics of multiple processes in the hydrodynamic model depend in different ways on the specific physical content of the above stages of the process. Comparison of the model with experiment may therefore throw light on the validity of the hydrodynamic description at different stages of the process.[77]

Let us consider this statement in greater detail. The choice of the initial volume will largely determine the behavior of the mean multiplicity $\langle n(E_0)\rangle_A$ as a function of primary energy E_0 and the number A of nucleons in the nucleus. Hydrodynamic outflow determines the distribution of secondary particles over the rapidities, i.e., dn/dy. The final stage determines the shape of the distribution of secondary particles over the transverse momenta, $dn/dp_\perp$, and their abundance. Studies of the various characteristics will, therefore, essentially "verify" the different stages of the hydrodynamic approach.

Let us now summarize the main quantitative predictions of the hydrodynamic theory for $c_0^2 = 1/3$, which corresponds to a perfect ultrarelativistic gas. It is precisely for this equation of state that the theory is in good agreement with experiment.[77]

a) The multiplicity of secondary particles is given by[80]

$$\langle n(E_0)\rangle_A \sim E_0^{1/4}A^{\alpha}, \tag{14}$$

where $\alpha \approx 0.15 - 0.20$.[11)]

b) The distribution in the rapidity y^* in the center-of-mass system for $n_{tube} < 3.7$[81] is:

$$\frac{dn}{dy} = \langle n\rangle (2\pi\mathcal{L})^{-1/2}\exp\left[-\frac{(y^*)^2}{2\mathcal{L}}\right], \tag{15}$$

$$\mathcal{L} = 0.56\ln\frac{E_0}{M} + 1.6\ln\frac{n_{tube}+1}{2} + 1.6, \tag{16}$$

where $\langle n\rangle \approx \langle n_s\rangle$ is the mean multiplicity (largely shower particles), n_{tube} is the number of nucleons in the tube and is given by $n_{tube} \sim A^{1/3}$, M is the nucleon mass, and E_0 is the nucleon energy in the laboratory system.

c) When $n_{tube} > 3.7$, the angular distributions of the secondary particles should be asymmetric in the center-of-mass system. This occurs because of the asymmetry of the initial conditions (mass of tube $M_{tube} \approx MA^{1/3} \neq M$). On average, more particles are emitted in the direction of motion of the tube (region of fragmentation of the nucleus) as compared with the direction of motion of the primary nucleon. The velocity v_c of the center-of-mass system relative to the equal-velocity system in which the emission is symmetric is given by[82]

$$v_c = \mathrm{th}\left[\frac{\sqrt{3}}{2} + \frac{2n_{tube}-4-2\sqrt{3}}{7+4\sqrt{3}} - \mathrm{Arth}\left(\frac{n_{tube}-1}{n_{tube}+1}\right)\right]. \tag{17}$$

Therefore, the y^* distribution for $n_{tube} > 3.7$ has the form

$$\frac{dn}{dy^*} = \langle n\rangle (2\pi\mathcal{L})^{-1/2}\exp\left[-\frac{(y^*-y_c)^2}{2\mathcal{L}}\right], \tag{18}$$

$$y_c = \mathrm{Arth}\, v_c. \tag{19}$$

d) The $p_\perp$ distribution is determined largely by thermal motion. For $E_0 \lesssim 10^{13}$ eV, this assumption is fully justified[83] and, if it is, then

$$\frac{dn}{dp_\perp^2} \sim \sum_{r=1}^{\infty}(\pm 1)^{r-1}K_1\left[r\sqrt{1+\left(\frac{p_\perp}{\mu}\right)^2}\right]. \tag{20}$$

In this expression, $K_1(x)$ is the Bessel function of an imaginary argument and the positive and negative signs correspond to fermions and bosons, respectively. When the three-dimensional character of the hydrodynamic outflow is taken into account, this leads to the appearance of a weak dependence of the mean transverse momentum $\langle p_\perp\rangle$ on E_0:

$$\langle p_\perp\rangle \sim E_0^{1/15}. \tag{21}$$

e) The abundance of secondary particles for $n_i \gg 1$

[11)] It is frequently assumed that $\alpha \approx 0.19$, but this estimate is obtained as a result of averaging over all the collision parameters (including the periphery of the nucleus). This procedure is not, however, good enough to enable us to calculate α to better than 0.01.

(i labels the type of particle) is determined by statistical thermodynamics (see, for example, [84]):

$$\langle n_\pi \rangle : \langle n_K \rangle : \langle n_{\bar{p}} \rangle \simeq 1 : 0.1 : 0.01. \tag{22}$$

When $\langle n_i \rangle \ll 1$ $(i = K, \bar{p})$

$$\langle n_i \rangle \sim \langle n_\pi \rangle^2. \tag{23}$$

f) Conservation laws clearly show that the tube model implies the existence of pions (hadrons), the velocity of which in the center-of-mass system exceeds the velocity of nucleons in the nucleus (or of the incident hadron).

We are now in a position to compare the predictions of the model with experimental results (see Chap. 1).

The dependence of $\langle n_s \rangle$ on A is not inconsistent with (14) (see Sec. 1.1 and Fig. 3). The y^* distribution is satisfactorily described by (15) and (18) (see Sec. 1.2). This agreement has been demonstrated in[24] (see Fig. 7).

The $p_\perp$ distribution depends only very slightly on the primary energy of incident and generated particles, in accordance with hydrodynamic theory; the quantity $\langle p_\perp \rangle$ increases with increasing mass of the secondary particle (see Sec. 1.6). Experiment reveals the presence of pions with energies exceeding the center-of-mass energy per nucleon in the nucleus.

The emission of secondary hadrons exhibits an asymmetry. There are more hadrons in the nuclear fragmentation region than in the region of fragmentation of the incident particle (see Sec. 1.2).

Within the framework of the hydrodynamic picture, the number of secondary nucleons is determined by the total transverse momentum transferred to the nucleus and by the properties of nuclear matter. Since the value of n_{tube} is practically independent of E_0, the number N_h should not depend on E_0, and this appears to be in agreement with experimental data (see Sec. 1.3 and Fig. 9).

The most important characteristics of hadron-nucleus interactions at high energies are thus satisfactorily described by the tube model in its hydrodynamic interpretation.[12)]

We note in conclusion that the above comparison with experiment was carried out for sound velocity $c_0 = 1/\sqrt{3}$. At present, experimental data are not accurate enough to exclude possible changes in c_0 by 0.1 (see, for example, [24]).

2.7. The Gottfried model

A somewhat unusual hydrodynamic-type model has recently been put forward[85] for the hadron-nucleus interaction. It can be described as "inverted hydrodynamics." The starting points in this model are the experimental data on $\langle n(E_0) \rangle \approx \langle n_s \rangle$ and dn/dy. It is assumed that, at high energies, $\langle n_s \rangle \sim \ln s/M^2$ and $dn/dy = \text{const}$. The hydrodynamic approach is adopted in this model to deduce the development of the interaction with the nucleus along the time axis. It is assumed that the elements of the hadronic fluid move along classical trajectories, in accordance with the equations of relativistic hydrodynamics, and the initial conditions for this motion are chosen so that the above behavior of $\langle n_s \rangle$ and dn/dy is satisfied.

The basic postulates of the model can be formulated as follows. The first collision of the hadron with a nucleon in the nucleus results in the formation of a material consisting of several elements which are distributed over rapidities in the same way as in the collision between a hadron and a free nucleon (in the first approximation, $dn/dy = \text{const}$). At this time, the emerging elements are not identical with real particles. They can be said to be systems similar to the elements of a fluid in the hydrodynamic model. These elements subsequently interact with the remaining nucleons and the cross section for this is equal to the cross section for the interaction between hadrons and free nucleons.

The characteristic parameter of the process is the Lorentz factor of an element (equivalent to the hydrodynamic velocity), i.e., the ratio of the lifetime τ of the element in the center-of-mass system to the lifetime τ_0 in its own frame. The number of elements increases with increasing value of τ/τ_0 but is always less than the number of real hadrons. The next step is that the elements of the resulting system interact with the second, third, and so on, nucleons in the tube. The net effect is obtained as a result of the superposition of collisions in the tube and averaging over all the chords of the nucleus.[13)] This procedure leads to the following expression:

$$\langle n(s, A) \rangle = \langle n(s, 1) \rangle \left[1 + \tfrac{1}{3} (\nu_A - 1) \right], \tag{24}$$

where $\langle n(s, 1) \rangle$ is the mean multiplicity in a hadron-nucleon collision and $\nu_A \sim A^{1/3}$ is the mean number of collisions in the nucleus of mass number A. This formula is in agreement with experimental data (see Sec. 1.1 and Fig. 3).

We note that the Gottfried model is an *ad hoc* procedure developed to explain the behavior of $\langle n(s, A) \rangle$. However, it is based on the conclusion that traditional hydrodynamic theory does not provide a correct description of experimental results and this, in turn, is based on the incorrect expression (see[74])

$$\langle n(s, A) \rangle = \langle n(sn_{\text{tube}}, 1) \rangle, \tag{25}$$

which does not take into account the increase in the mass of the tube as A is varied. The correct expression given by the hydrodynamic model is $\langle n(s, A) \rangle = \langle n(sn_{\text{tube}}, n_{\text{tube}}) \rangle$, and this leads to (14) instead of the in-

[12)] We note that it is stated in[6] that the tube model is in conflict with experimental data. This conclusion is based on a misunderstanding because the comparison carried out in[6] corresponds to energies $E_0 \lesssim 10$ GeV for which this model is definitely unsatisfactory.

[13)] See[86] for the latest information about this model.

correct result $\langle n\rangle \sim A^{1/12}$, given in[74]. The presumption made in[74,85], namely, that the accepted variant of the hydrodynamic model, summarized in Sec. 2.6, has to be modified is thus no longer valid. Since the Gottfried model does not explain the hadron-nucleon interaction but takes its parameters from experiment or other theoretical sources, it is even less general than the Landau hydrodynamic model. Moreover, the discussion given in[86] emphasizes that the Gottfried model is not relativistically invariant (in contrast to the hydrodynamic model).

2.8. Hydrodynamic interpretation of the interaction of high-energy photons and leptons with nuclei

The hydrodynamic theory has been successfully used to interpret the process $e^+e^- \to h^+, \ldots$ (see[87,88] and the review given in[89]). There is, therefore, a general tendency to try and generalize the hydrodynamic approach to the case of collisions of leptons (l) and photons (γ) with nuclei:

$$\gamma + A \to h + X, \tag{26}$$
$$l + A \to l + h + X, \tag{27}$$

where X is the system of "undetected hadrons." This approach is based on a certain equivalence between a real photon γ or a virtual photon γ^* and a hadron (see Sec. 1.7). In fact,[90,91] as a result of virtual transitions, the photon γ (or γ^*) spends some of its life in the form of hadrons. The lifetime of the "hadronic states" of a photon can be estimated from the uncertainty principle

$$\tau \Delta E \sim 1, \tag{28}$$

where ΔE is the difference between the energies of the photon and the hadronic system for equal momenta. At high energies:

$$\Delta E_\gamma = \sqrt{E_\gamma^2 + m^2} - E_\gamma \approx \frac{m^2}{2E_\gamma}, \tag{29}$$
$$\Delta E_{\gamma^*} = \sqrt{(E_{\gamma^*})^2 + m^2 + Q^2} - E_{\gamma^*} \approx \frac{m^2+Q^2}{2E_{\gamma^*}}, \tag{30}$$

where $Q^2 = -q^2 > 0$, q^2 is the square of the 4-momentum transferred to the nucleus (tube), and m is the mass of the virtual hadronic state.

The time during which the photon behaves as a hadron (or hadrons) increases with increasing energy:

$$\tau_\gamma \sim \frac{2E_\gamma}{m^2}, \tag{31}$$
$$\tau_{\gamma^*} \sim \frac{2E_\gamma}{m^2+Q^2}. \tag{32}$$

If the range of virtual hadrons into which the photon $\gamma(\gamma^*)$ has decayed is greater than the range of a hadron in the course of its interaction with nuclear matter, the photon γ (or γ^2) will efficiently interact with the nucleus through its hadronic field. In other words, the interaction of the γ (or γ^*) photon can be treated in terms of the interactions of hadrons. The conditions for the validity of this approach are defined by the inequalities

$$E_\gamma \gg \frac{m^2}{\mu}, \tag{33}$$
$$E_{\gamma^*} \gg \frac{m^2+Q^2}{\mu}. \tag{34}$$

The collision between a γ (or γ^*) and a nucleus can then be looked upon as a collision with a tube with transverse size μ^{-1}. The direction of $\mathbf{p}$ (or $\mathbf{p}_{\gamma^*}$) is to be taken as the collision axis.

To begin with, we shall consider real photons. The most bothersome question arises in the choice of the initial volume. This is so because, in the case of a γA (or $\gamma^* A$) collision, the incident particle (γ, e, μ) does not have a characteristic volume (for the γ ray, even the equal-velocity system is not available).

We shall adopt two alternative assumptions with regard to the initial volume[92]:

(a) The initial volume is equal to the compressed volume of the tube in the center-of-mass system (as in the case of hA collisions for $n_{\text{tube}} < 3.7$).

(b) The initial volume is equal to the uncompressed volume of the tube in the laboratory system ($V \sim \pi n_{\text{tube}} \times \mu^{-3}$). Certain essentially model estimates[93] suggest this possibility.[14)]

Next, let us consider the ambiguity in the choice of the initial volume. Roughly speaking, the initial volume determines the function $\langle n_s(s, A)\rangle$, and its shape determines the functions dn/dy and $dn/dp_\perp$. The abundance of secondary hadrons, which is determined only by the final temperature T_f, is the characteristic that is the least sensitive to the choice of the initial volume. For variant (a), we can use all the expressions obtained previously for hA collisions [$\langle n_s(s, A)\rangle$, $\langle p_\perp(s, A)\rangle$, etc.].

A different form is obtained for the functions $\langle n_s(s, A)\rangle$ and $\langle p_\perp(s, A)\rangle$ in the case of variant (b):

$$\langle n_s \rangle \sim s^{3/8} A^{1/12}, \tag{35}$$
$$\langle p_\perp \rangle \sim s^{1/8} A^{-1/12}, \tag{36}$$

where $s \approx 2M_{\text{tube}} E_\gamma$. It is important to note that the values of $\langle p_\perp\rangle$ are now very dependent on s. The predictions of the model with regard to lA interactions for $Q^2 \lesssim M^2$ are the same as the prediction for γA collisions provided E_γ is replaced by E_{γ^*} and $\mathbf{p}_\gamma$ by $\mathbf{p}_{\gamma^*}$. Existing data on interactions of high-energy photons and leptons with protons, deuterons, and nuclei (see Sec. 1.7) are not very voluminous, but they do indicate that $\langle p_\perp\rangle$ is independent of s and the numerical value $\langle p_\perp\rangle \sim 350$ MeV/c is in agreement with the measured value for hN and hA collisions. Thus, if the hydrodynamic model can, in fact, be used to describe lA and γN interactions, this can only be done by adopting assumption (a). From the point of view of verifying the generality of the entire idea, the most important is the verification of the universality of the functional form of

---

[14)] It is noted in[94] that the longitudinal size of the interaction region may even increase with increasing energy in the deeply inelastic region.

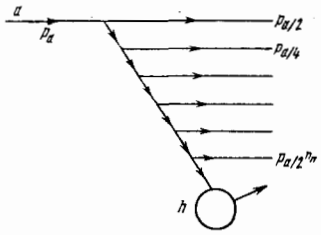

FIG. 23. Decay of a hadron a into partons. The slow parton with momentum $p_p \sim p_a/2^{n_p}$ interacts with the target hadron h (n_p is the number of partons).

$\langle n_s(s, A)\rangle$, $\frac{dn}{dy}(s)$, $\frac{dn}{dp_\perp}(s)$,

the abundance, and so on.

2.9. Space-time picture of the interaction with a nucleus in the parton model

a) Assumptions ot the parton model. The parton model of hadrons[91,95] is, at present, the foundation for the qualitative analysis of the deeply inelastic lepton-hadron interaction and the hadron-hadron interaction processes. We must recall the basic assumptions of this model, which are important for the understanding of our subsequent discussion. In the parton picture, it is assumed that:

1) A free hadron moving along the z axis with high momentum $p_h \gg m_h$ (m_h is the hadron mass) undergoes a virtual dissociation into a system of point particles called partons.

2) The lifetime of a parton belonging to this fluctuation is $\tau_p \sim E_p m_p^{-2}$, where E_p is the parton energy and m_p its effective mass ($m_p \sim 1$ GeV).

3) The fact that partons are points ensures that the interaction between them is relatively weak. Only partons with small relative momenta ($p_p^* \sim m_p$) interact strongly. The upper limit for the total parton-parton (or parton-hadron) cross section is determined from the unitarity condition for the interaction amplitude in the s state:

$$\sigma(\text{parton} + \text{parton} \to \text{all}) \leqslant 4\pi\lambda_p^2, \tag{37}$$

where $\lambda_p = (p_p^*)^{-1}$ is the parton wavelength in the center-of-mass system of the colliding partons and p_p^* is the parton momentum in this system.

4) Because of the small probability of an interaction between partons belonging to a given ultrarelativistic hadron, the parton spectrum for $x \ll 1$ is $f(x) \sim dx/x$ where $x = p_p^*/p_h^*$. Experimental data on deeply inelastic ep interactions show that, as $x \to 1$, the spectrum of partons inside a nucleon decreases rapidly, in accordance with the expression $f(x \to 1) \sim (1-x)^3$. Partons with momenta $p_p \sim m_p$, and partons traveling in the direction opposite to that of the momentum of the hadron to which they belong, are practically absent from the parton spectrum of the hadron.

5) The transverse momenta $p_{p\perp}$ of the partons are restricted by the inequality $\langle p_{p\perp}\rangle \sim m_p$, i.e., they do not increase with increasing hadron energy.

The interaction between an ultrarelativistic hadron a and a hadron h at rest can be described graphically within the framework of the parton idea as shown in Fig. 23. The hadron a decays successively into two partons with momenta $p_a/2$ (this value is chosen for simplicity and is not of any great significance), one of the resulting partons again decays into two partons with momenta $p_a/4$, and so on. Only the slowest parton belonging to the fluctuation and having momentum $p_p \sim m_p$ interacts with the target hadron h in Fig. 23. The partons can subsequently transform into hadrons (multiple production) or can again assemble into a hadron a (elastic scattering), but the latter event is of low probability.[95] The model given in Fig. 23 can readily be used to estimate the number of successive decays. After the n_p-th decay, the parton momentum is $p_a/2^{n_p}$ and the subdivision process continues until the momentum of the slow parton has the order of magnitude $p_p \sim m_p$, after which the slow parton interacts with the target hadron h. Thus, $p_a/2^{n_p} \sim m_p$ and hence

$$n_p \sim \ln \frac{p_a}{m_p}. \tag{38}$$

The size of the parton fluctuation in the transverse direction is[95] [15)]

$$\rho_\perp \sim m_p^{-1} \sqrt{\ln \frac{p_a}{m_p}}. \tag{39}$$

Next, since the reassembly of partons into the initial hadron, after the interaction of the slow parton with the target hadron h (elastic scattering), is of low probability (in agreement with experiment), the question arises as to how many hadrons can be created as a result of the transformation of partons into hadrons? It seems very likely that the mean multiplicity $\langle n\rangle$ of hadrons should be proportional to the number of partons in the fluctuation (see Fig. 23):

$$\langle n\rangle \sim n_p \sim \ln \frac{p_a}{m_p}, \tag{40}$$

which is in agreement with the predictions of multiperipheral models and is not in conflict with experimental data.

b) Coalescence of "soft" partons in the nucleus and deeply inelastic interactions between leptons and nuclei.[16)]

We now apply the parton model to the interaction between hadrons (photons) and nuclei.

The distribution function for partons inside a nucleon can be determined as a result of experiments on deeply inelastic eN or $\nu_\mu N$ interactions. The deeply inelastic interaction process can be described within the framework of the parton picture as the absorption of a virtual

[15)] Fluctuations of virtual particles in the transverse direction were first discussed in[96].

[16)] This and the subsequent sections are based on the results in[97-100].

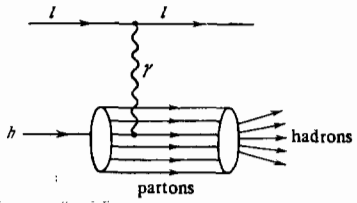

FIG. 24. Diagram illustrating the absorption of a virtual γ photon (emitted by the lepton l) by one of the partons, into which the fast hadron h has decayed. Lower right-hand side of the diagram symbolizes the unknown mechanism responsible for the transformation of partons into hadrons.

γ (W boson) by a point parton in a nucleon, followed by the transformation of the system of partons into real hadrons (Fig. 24).

Since the parton idea is defined in the frame in which the nucleon momentum is sufficiently high,[91] we shall consider the absorption of the γ photon (W boson) in the frame in which the nucleon has a sufficiently high momentum $p \gg M$ (M is the nucleon mass).

Neglecting the transverse motion of partons, and denoting the 4-momentum of the primary parton by $p_p = xp$, where p is the 4-momentum of the nucleon, we have $(p_p - q) = p_p'$, where p_p' is the 4-momentum of the secondary parton, or

$$Q^2 = 2p_p q = 2xM\nu, \tag{41}$$

where ν is the energy of the virtual γ photon (or W boson) in the laboratory system, $Q^2 = -q^2$, and q is the 4-momentum of the γ^* photon (W).

It follows from (41) that the γ^* photon (W boson) is absorbed by a certain definite parton carrying the following fraction of the longitudinal momentum of the nucleon:

$$x = \frac{Q^2}{2M\nu}. \tag{42}$$

On the other hand, in the case of an interaction with the nucleus, we have to establish which particular nucleon in the nucleus (in the frame in which the nucleus moves with relativistic velocity) contains the parton which has absorbed the γ^* photon (W boson). This can be determined qualitatively from the uncertainty principle. Thus, if the longitudinal momentum of the parton is $p_{p\parallel} = x|\mathbf{p}|$ ($\mathbf{p}$ is the 3-momentum of the nuclear nucleon), the parton will, in accordance with the uncertainty principle, be localized in the longitudinal direction, as follows:

$$\Delta z \leqslant x^{-1}|\mathbf{p}|^{-1}. \tag{43}$$

In the rest frame of the nucleus, the separation between nucleons in longitudinal and transverse directions is $\Delta z_{12}^0 \sim \mu^{-1}$ and $\Delta\rho_{12} \sim \mu^{-1}$, respectively. In the moving frame, the longitudinal separations are reduced by the Lorentz factor γ ($\gamma \approx |\mathbf{p}|/M$), where M is the nucleon mass and

$$\Delta z_{12} \sim \frac{M}{\mu|\mathbf{p}|}. \tag{44}$$

When $\Delta z_{12} \leqslant \Delta z$ (see[98]), partons characterized by the values

$$x \leqslant \frac{\mu}{M}, \tag{45}$$

belong simultaneously to two neighboring nucleons in the nucleus. Since the relative momenta of these partons are sufficiently small, they interact relatively strongly, and this gives rise to the coalescence of the partons. According to the fundamental hypothesis of the parton model, a universal equilibrium distribution of partons belonging to two neighboring nucleons in the nucleus should then be established for small values of x and should be of the form[17)]

$$dn_p(x) \sim \text{const} \cdot \frac{dx}{x}. \tag{46}$$

The coalescence process ensures that the density of partons with $x \lesssim \mu/M$ turns out to be the same as that of an individual nucleon. This situation forms the basis for the application of the parton model to the quantitative analysis of hadron-nucleus interactions. In field-theoretical language, the simplest variant with interaction Lagrangian $Z_{\text{int}} = \lambda\varphi^3$ is that in which the parton coalescence process can be described as the coalescence of two parton coalescence of two parton "combs" belonging to neighboring nucleons (Fig. 25) into a single comb, beginning with a certain value of $x = x_0 \sim \mu/M$. In Fig. 25, two partons with momenta equal to one unit coalesce into a parton having a momentum of two units which, after decay, forms a parton "comb" with smaller values of momenta, i.e., 1, 1/2, 1/4, and so on.

Thus, the coalescence of parton fluctuations of neighboring nucleons begins for $x \lesssim x_0$. As x decreases, the localization of partons in the transverse direction may exceed the nuclear size: $\Delta z \lesssim RM/|\mathbf{p}|$, where R is the nuclear radius in the rest frame. This will occur for

$$x \leqslant (RM)^{-1} \sim x_0 A^{-1/3}. \tag{47}$$

When this inequality is satisfied, parton fluctuations of nucleons in the nucleus with the same transverse coordinates will cross in the longitudinal direction. Because of the parton coalescence process, the density of any distribution of such partons in x turns out to be the same as for an individual nucleon.

Let us now calculate the number of nucleons whose partons have coalesced for $x \lesssim x_0 A^{-1/3}$ into a single comb. The density of nucleons in the moving nucleus is

$$d \sim A\left(\frac{4\pi}{3}R^3\frac{M}{|\mathbf{p}|}\right)^{-1}.$$

The volume of the part of the nucleus in which the parton coalescence has taken place in the longitudinal direction is $V \sim \pi\rho^2 RM/|\mathbf{p}|$. Hence, we find that the num-

[17)] This distribution is closely related to the hypothesis of scaling invariance (see[91]).

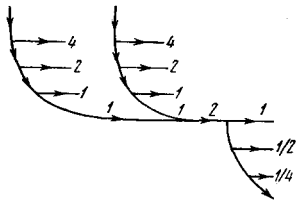

FIG. 25. Coalescence of two parton combs. Numbers indicate relative parton momenta.

ber of nucleons whose partons have coalesced is $n \sim \rho_\perp^2 R/r_0^3$, where $\rho_\perp$ is the transverse size of the parton fluctuation [see (39)], $R = r_0 A^{1/3}$ and $r_0 \sim \mu^{-1}$. The number of soft partons in the nucleus with $x \lesssim x_0 A^{-1/3}$ is reduced by a factor of $\bar{n}$ as a result of the coalescence process, i.e., the effective number of nucleons in the nucleus during the interaction process characterized by $x \lesssim x_0 A^{-1/3}$ is of the order of[98]

$$N_{\text{eff}} \sim \frac{A}{\bar{n}} \sim A^{2/3}, \tag{48}$$

where $\rho_\perp \lesssim \mu^{-1}$. This means that, for example, the total cross section for the interaction between a nucleus and a hadron (photon, W boson) for $x \lesssim x_0 A^{-1/3}$ is given by (see Sec. 1.4)

$$\sigma_{\text{tot}} \sim A^{2/3}. \tag{49}$$

For $x_0 A^{-1/3} \lesssim x \lesssim \mu/M$, instead of the effective number of partons, which is characteristic for the diffraction region (47), the parton model predicts an increase in the number of partons. Thus, Fig. 25 shows the coalescence of two combs and, if the combs were not to coalesce, we would have two partons with momenta of one unit each. The coalescence of two combs results in the appearance of a parton with momentum of two units (Fig. 25) which, after decay, produces one further parton with momentum 1 and partons with momenta 1/2, 1/4, and so on. In the final state, there are three partons with momenta 1, and not two, as in the case of two noncoalesced "combs." This has been called the antiscreening effect.[98]

c) Multiple production of hadrons on nuclei. The multiple production of hadrons on nuclei is usually considered in the laboratory system in which the nucleus is at rest. We shall follow this tradition but, whenever necessary, we shall emphasize the relation between the predicted phenomena and the spatial distribution of partons in the nucleus, which we have previously considered in the frame in which the nucleus is at rest.

Multiperipheral (multireggeon) models suggest that the shower particles (n_s) are largely fragments of the incident hadron which are created outside the nucleus or on its periphery. These particles are formed as a result of the transformation of partons emitted by the incident hadron into secondary hadrons.

Such partons have momenta

$$p_p \gtrsim R m_p^2 \sim m_p x_0^{-1} A^{1/3} = p_{\text{crit}} \tag{50}$$

and can propagate in the longitudinal direction to distances

$$\Delta z \sim \tau_p c \sim \frac{p_p}{m_p^2} \gtrsim R, \tag{51}$$

which exceed the size of the nucleus. The shape of the spectrum of such partons in momentum space and, correspondingly, the spectrum of hadrons into which they are transformed, is independent of the nuclear parameters, and is the same as the spectrum of hadrons created in collisions with free nucleons. The cross section for the interaction of partons having momenta given by (50) with nucleons is very small, in accordance with the basic postulate of the parton model [see (37)]. These partons correspond in the antilaboratory system (in which the nucleus is in motion) to partons which are common to all the nucleons in the nucleus in a tube with transverse size $\rho_\perp \sim \mu^{-1}$ ($x \lesssim x_0 A^{-1/3}$). As already noted, these partons provide the main contribution to the diffraction mechanism of the interaction. In this part of the spectrum, the shape of the inclusive distribution of secondary hadrons is no different from the spectrum produced during a collision with free nucleons. Such hadrons ($p > p_{\text{crit}}$) are called fast shower particles.[98] If the energy E_0 of the incident hadron begins to exceed $E_{\text{crit}} \approx p_{\text{crit}}$, the energy available to the partons which can strongly interact with nucleons in the nucleus ceases to increase. This means that, for $E_0 > E_{\text{crit}}$, we should see the onset of a phenomenon which was referred to in[98] as the limiting fragmentation of the nucleus.[18] This is meant to describe a situation in which the energy spectra of "gray" and "black" particles, and the distributions over the multiplicities, the correlations between secondary particles, and other characteristics of hadron-nucleus interactions cease to depend both on the energy of the incident particle and on its species. This property is also exhibited by shower particles with momenta $m_p x_0^{-1} \lesssim p \lesssim p_{\text{crit}}$, which originate from partons and interact relatively strongly with nucleons in the nucleus, giving rise to the breakup of the latter. Such particles can be referred to as slow shower particles. In the antilaboratory system, slow shower particles are produced from partons with $x_0 A^{-1/3} \lesssim x \lesssim x_0$. For $E_0 > E_{\text{crit}}$, the inclusive spectra of the slow shower particles and the correlations between their multiplicities and the multiplicities of gray and black particles with $p \lesssim m_p x_0^{-1}$ cease to depend on E_0 and on the species of the incident particle a. This is also valid for the correlations between the multiplicities of fast shower particles and "gray" and "black" particles.

Experimental evidence, of which there is very little, is in general agreement with the above predictions (see Chap. 1 and Figs. 3, 6, 7, and 9).

We note in conclusion that the main qualitative predictions of the parton model insofar as the multiple creation on nuclei is concerned can be summarized as follows:

---

[18] We note that an analogous term was introduced in[101], where the formation of cumulative protons and deuterons on nuclei was discussed, i.e., an effect physically different from that discussed in[98].

1) For energies $E_0 \lesssim m_p x_0^{-1} A^{1/3} \sim 10 A^{1/3}$ GeV ($x_0 \sim 0.05$, $m_p \sim 1$ GeV), one should be able to observe the phenomenon of limiting fragmentation of the nucleus in the sense defined in[98]. In this region, all the characteristics of the nuclear cascades cease to depend on energy and on the species of the primary particle. This prediction is verified by experiment (see Sec. 1.1 and Fig. 9).

2) The multiplicity of fast shower particles is estimated by

$$\langle n_{sf} \rangle \approx \text{const} \cdot \int_{m_p/E_0}^{x_0 A^{-1/3}} \frac{dx}{x} \approx \text{const} \cdot \ln\left(\frac{E_0 A^{1/3}}{m_p x_0}\right), \tag{52}$$

where the constant on the right-hand side of this equation is, in fact, a universal constant for all nuclei because the spectrum of soft partons is universal for $x \lesssim x_0 A^{-1/3}$ for all nuclei in the antilaboratory system.

The shape of the inclusive spectrum of fast shower particles is the same as the shape of the inclusive spectrum on the nucleon target in the region of fragmentation of the incident particle, i.e., $dn_A/dy \approx dn_N/dy$. This is also verified by experiment (see Figs. 6 and 7).

3) The multiplicity of slow shower particles[98] is a function of A, as follows:

$$\langle n_{sc} \rangle \sim \tilde{n} \sim \text{const} \cdot A^{1/3}, \tag{53}$$

where $\tilde{n}$ is the number of nucleons in which the clouds of partons with $x_0 A^{-1/3} \lesssim x \lesssim x_0$ are found to overlap (see Sec. b) and there is, therefore, enrichment with partons due to their coalescence. As noted in[98], if we take into account the interaction between partons in the final state, the dependence of $\langle n_{sc} \rangle$ on A may turn out to be much weaker than indicated by (53).

4) The boundedness of $\langle p_\perp \rangle$ is postulated right from the outset in the parton model. The very essence of the model is that $\langle p_\perp \rangle$ should not depend on A, and this is in agreement with existing data (see Sec. 1.6).

5) The parton model predicts that the function $\langle n_s(A) \rangle$ will have a different shape in different regions of the spectrum in x. According to 2), the multiplicity of fast shower particles, $\langle n_{sf} \rangle$, is a very slow (logarithmic) function of A. The multiplicity of slow shower particles is $\langle n_{sc} \rangle \sim A^{1/3}$ according to 3) or, perhaps, an even slower function of A because of the interaction between partons in the final state.[98] On the average, one would expect in this part of the spectrum a relatively slowly-varying function $\langle n_s(A) \rangle$, and this is in qualitative agreement with experimental data (see Sec. 1.1 and Fig. 3).

6) We have not discussed in this paper the complicated problem of emission of several parton combs at once by the primary hadron. This effect should lead to an increase in the multiplicity of shower particles during the interaction between hadrons and nuclei at high energies.[99]

We note in conclusion that the parton model has given rise to a whole series of problems which will have to be tackled in the future both theoretically and experimentally. Thus, firstly, the quantity x_0, which is critical for the coalescence of "soft" partons inside the nucleus, may turn out to be very small ($x_0 \approx 0.03 - 0.05$[98,100]). Most of the effects discussed above will then appear only at very high energies.

Secondly, existing data on the formation of hadrons with high $p_\perp \gtrsim 2$ GeV/c suggest that the differential cross section for the creation of such hadrons on nuclei is invariant, $Ed^3\sigma_A/d^3p \sim A^{1.1-1.2}$ (see Sec. 1.6 and Fig. 15). Within the framework of the parton picture, such hadrons should appear as a result of collisions between relatively hard partons belonging to the incident hadron and nucleons in the nucleus. The nucleus is transparent to such partons, and one would expect $Ed^3\sigma_A/d^3p \sim A$.

The most difficult and, at the same time, the most important problem is to make the parton model as quantitative as possible for hadron-hadron and hadron-nucleus interactions. Some successful attempts in this direction have already been reported[100] and have demonstrated that it is possible to obtain an approximate (to within 20–30) description of existing data (see Chap. 1) on the dependence of dn/dy and $R_A = \langle n(E_0, A) \rangle / \langle n(E_0, A) \rangle$ on E_0 and A for shower particles.[19)]

Finally, we note the paradoxical similarity between the predictions of the hydrodynamic and parton models which impedes the experimental separation of these predictions. This is due to the quasi-one-dimensional treatment of the partons and of the hadronic fluid in hydrodynamics, and also the Lorentz dilatation of the lifetime of the elements of the system. In both cases, $\tau \sim E/m^2$.

CONCLUSIONS

Experimental and theoretical studies of the interactions between fast particles and nuclei have led us to a certain qualitative picture of the space-time development of hadronic fields during the interaction. The spatial region in which the interaction takes place has linear dimensions exceeding those of the nucleus. This leads us to a new kind of physics in the sense that the nucleus appears as the analyzer of the evolution of the virtual phase in space-time. This picture is still far from being complete. Nevertheless, one would hope that further studies of this question will illuminate important facets of the strong interaction. With this aim

---

[19)] A calculation concerned with the cascade of parton interactions with intranuclear nucleons is reported in[100]. It is important to emphasize that the physics underlying the model used in[100] is radically different from the traditional cascade model (see Sec. 2.5). The authors of[100] estimate the transformation of virtual particles (partons), whose interaction with nucleons and with one another has nothing in common with the interaction between real hadrons. However, the methodology of calculations concerned with the parton shower is similar to that employed in treating cascades of real hadrons.

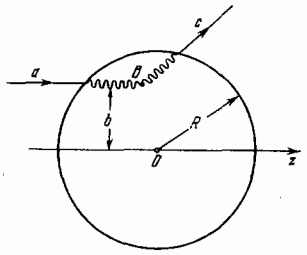

FIG. 26. Calculations on the interaction between a hadron a and a nucleus in which a hadron c is produced. Wavy line indicates that hadrons a and c are subject to absorption in the interior of the nucleus. B—point of creation of secondary hadron c; R—mean radius of the nucleus; O—center of gravity of the nucleus; b—impact parameter; the z axis is parallel to the direction of motion of the incident hadron.

in view, we may sketch out the following very preliminary program for further studies:

1. Detailed investigation of the functions $\langle n(E_0, A)\rangle$, $Ed^3\sigma/d^2p$, dn/dy, $dn/dp_\perp$, and $K(A)$ on different nuclear targets. In particular, it would be interesting to investigate $dn/dp_\perp(A)$ for $p_\perp \gtrsim 2$ GeV/c.

2. It is very important to verify the universality of these distributions (or the absence of this universality) for different types of incident particle ($p, n, \pi, K, \bar{p}, \gamma, l$, etc.).

3. It is very interesting to consider the abundance of particles produced on different targets and for different incident particles. For example, a confirmation of an increase of $\langle p_\perp\rangle$ with E_0 would be evidence in favor of hydrodynamic-type models. Verification of the universality of the distributions would indicate the importance of the final stages of the process.

All these questions are beginning to be studied or are still practically blind spots. When multiple processes are investigated on nuclei, it is important to employ methods that are relatively new in this part of physics, namely, magnetic spectrometers, large bubble chambers filled with heavy materials (Ne, Xe), and so on.

From the theoretical point of view, it will be important to develop further the field-theoretical approach (parton model), to improve the concept of clusterization, and to carry out more rigorous comparison between theoretical models (for example, the tube model) and experimental data.

It seems to us that it is essential, to begin with, to concentrate our attention on the dependence of the characteristics of relatively fast particles on A and on the energy, bearing in mind that the characteristics of slow particles are more dependent on the state of excited nuclear material than on the field of the incident elementary particles. The properties of nuclear matter at high pressures are, in themselves, of enormous interest (for example, in the light of the possible excitation of shock waves in the nucleus[102]), but this is a separate question which requires separate consideration.

APPENDIX

INELASTIC INTERACTION OF HADRONS WITH NUCLEI IN THE OPTICAL APPROXIMATION AND THE GLAUBER METHOD

We shall now give a simplified derivation of the dependence of the coherent and noncoherent cross sections for the production of hadrons on nuclei on the cross sections for the interaction of primary and secondary hadrons with nucleons inside the nucleus. We shall assume that the nucleus is a continuous nuclear medium with density $A\rho(r)$, where A is the number of nucleons in the nucleus. This is valid for intermediate and heavy nuclei when the mean range of a hadron in the nucleus is $\lambda \ll R$ (R is the nucleus radius). Suppose that the reaction

$$a + N \to c + N \qquad (A.1)$$

is characterized by the amplitude $f_{ac}(\mathbf{q})$ ($\mathbf{q}^2 \approx t'$) and takes place on a nucleon inside the nucleus for a certain value of the impact parameter b at a point with longitudinal coordinate between z and $z+dz$ (Fig. 26). Since, at high energies, elastic scattering is largly small-angle scattering, we shall assume that, up to the point where the reaction (A.1) takes place, the hadron a moves along a rectilinear trajectory. Similarly, it is assumed that the secondary hadron c will also move along a straight line (Fig. 26). This approach to the interaction with nuclei is commonly called the optical approximation. Let us consider the coherent production of a hadron c on the nucleus A. We must sum the amplitudes for the reaction (A.1) over all the possible impact parameters and all intervals Δz.

We shall have to take into account the fact that the number of target nucleons lying between z and $z+dz$ and between b and $\mathbf{b}+d\mathbf{b}$ is $dn = A\rho(\mathbf{b}, z)dzdb$. The wavefunction amplitude of the incident hadron will be reduced as a result of interactions preceding the reaction (A.1).

This reduction in the amplitude of the wavefunction of the primary hadron arriving at the point z and producing the reaction (A.1) is described by[20)]

$$\varkappa_a(\mathbf{b}, z) = \exp\left[-\frac{1}{2}\sigma_{aN}A\int_{-\infty}^{z}\rho(\mathbf{b}, z')\,dz'\right], \qquad (A.2)$$

where σ_{aN} is the total cross section for the aN interaction.

Similarly, for a secondary hadron c created at the point z, which subsequently traverses the nucleus, we have

$$\varkappa_c(\mathbf{b}, z) = \exp\left[-\frac{1}{2}\sigma_{cN}A\int_{z}^{\infty}\rho(\mathbf{b}, z')\,dz'\right], \qquad (A.3)$$

[20)]When the nuclear density is homogeneous for $0 \leqslant r \leqslant R$, the formula given by (A.2) leads to the obvious result: $\kappa_a = \exp(-l/2\lambda)$, where $l = \sqrt{R^2 - b^2} + z$ is the free path up to the reaction (A.1) and $\lambda = (A\rho\sigma_{aN})^{-1}$ is the mean free path of the hadron a in nuclear matter.

where σ_{cN} is the total cN interaction cross section.

To calculate the amplitude for the coherent process

$$a + A \to c + A \tag{A.4}$$

on the nucleus, we must multiply the amplitude for the process (A.1) on a bound nucleon, $f_{ac}(\mathbf{q})e^{i\mathbf{q}\cdot\mathbf{r}}$ ($\mathbf{r}$ is the coordinate of the nucleon in the nucleus), by factors representing the absorption of the incident and departing waves, $\varkappa_a$ and $\varkappa_c$, and by the number of nucleons in the element $dz d\mathbf{b}$. Finally, we must integrate over the entire volume of the nucleus. When these operations are completed, it is found that

$$F_{ac}(\mathbf{q}) = A f_{ac}(\mathbf{q}) \int d\mathbf{b} \int dz e^{i\mathbf{q}\mathbf{r}} \rho(\mathbf{b}, z) \varkappa_a(\mathbf{b}, z) \varkappa_c(\mathbf{b}, z). \tag{A.5}$$

The effective number of nucleons participating in the coherent process (A.4) is obviously given by

$$N_{\text{coh}} = A \int d\mathbf{b} \int dz e^{i\mathbf{q}\mathbf{r}} \rho(\mathbf{b}, z) \varkappa_a(\mathbf{b}, z) \varkappa_c(\mathbf{b}, z). \tag{A.6}$$

This formula can also be derived within the framework of the Glauber theory of multiple diffractional scattering by going to the limit of sufficiently heavy nuclei ($A \gg 1$, $R \gg \lambda$)[60,61] and by neglecting the real part of the amplitude for zero-angle elastic scattering of hadrons by nucleons (i.e., by neglecting the refraction of hadronic waves in nuclear matter).[61] We emphasize that the formulas given by (A.2) and (A.3) contain the total cross sections for aN and cN interactions because even the elastic scattering process leads to a violation of coherence.

We can use the same procedure to consider the noncoherent production of a hadron c on a nucleus A:

$$a + A \to c + A', \tag{A.7}$$

where A' is an excited nucleus or the products of nuclear fragmentation in the final state. Since the creation of a hadron c on nucleons inside the nucleus occurs in a noncoherent fashion, we must sum not the amplitudes but the cross sections for the creation of the hadron c between z and $z + dz$ and between $\mathbf{b}$ and $\mathbf{b} + d\mathbf{b}$. We must then take into account factors representing the absorption of primary (a) and secondary (c) hadrons which are, respectively, $\varkappa_a^2$ and $\varkappa_c^2$. The number of target nucleons in the elementary intervals dz and $d\mathbf{b}$ is, as before, $dn = A\rho(\mathbf{b}, z) dz d\mathbf{b}$. When all these factors are taken into account, it is found that the differential cross section for the noncoherent process (A.7) is given by[61]

$$\frac{d\sigma_{\text{incoh}}}{dt'} = A \frac{d\sigma_{ac}}{dt'} \int d\mathbf{b} \int dz \rho(\mathbf{b}, z) \varkappa_a^2(\mathbf{b}, z) \varkappa_c^2(\mathbf{b}, z), \tag{A.8}$$

where $d\sigma_{ac}/dt'$ is the differential cross section for the process (A.1) on an individual nucleon. It follows from (A.8) that the effective number of nucleons inside the nucleus, which participate in the noncoherent process, is given by

$$N_{\text{noncoh}} = A \int d\mathbf{b} \int dz \rho(\mathbf{b}, z) \varkappa_a^2(\mathbf{b}, z) \varkappa_c^2(\mathbf{b}, z). \tag{A.9}$$

We note, in addition, that the factors $\varkappa_a$ and $\varkappa_c$ now contain not the total cross sections but only the inelastic cross sections for the aN and cN interactions because elastic scattering does not attenuate the fluxes of incident and created particles. The formula given by (A.9) also follows from a more rigorous analysis of the corresponding expressions obtained on the basis of the Glauber method in the approximation of sufficiently heavy nuclei ($A \gg 1$, $R \gg \lambda$).[60]

The effective numbers of nucleons in the nucleus, N_{coh} and N_{noncoh}, are thus found to depend on the cross sections for the interaction between primary and secondary hadrons, on the one hand, and nucleons in the nucleus, on the other, and this enables us to obtain information about these cross sections from experimental data on coherent and noncoherent processes. A more rigorous derivation of the formulas of the optical approximation, and those of the theory of the Glauber multiple diffraction scattering with the production of hadronic resonances or hadronic systems with small multiplicity, can be found in.[62–64]

[1]V. S. Murzin and L. I. Sarycheva, Mnozhestvennye protsessy pri vysokikh energiyakh (Multiple Processes at High Energies). Atomizdat, M., 1974.
[2]Yu. P. Nikitin and I. L. Rozental', Teoriya mnozhestvennykh protesessov (Theory of Multiple Processes), Atomizdat, M., 1976.
[3]S. A. Slavatinskiĭ, Izv. Akad. Nauk SSSR Ser. Fiz. 39, 1172 (1975).
[4]C. B. A. McCusker, Phys. Lett. C 20, 229 (1975).
[5]V. S. Murzin and L. I. Sarycheva, Kosmicheskie luchi i ikh vzaimodeĭstvie (Cosmic Rays and Their Interaction), Atomizdat, M., 1968.
[6]V. S. Barashenkov and V. D. Toneev, Vzaimodeĭstvie vysokoénergeticheskikh chastits i yader s yadrami (Interaction of High-Energy Particles and Nuclei With Nuclei), Atomizdat, M., 1972.
[7]A. Gurtu, P. K. Malhotra, J. S. Mittra, *et al.*, Phys. Lett. B 50, 391 (1974).
[8]S. A. Azimov, Vo Van Tkhuan, *et al.*, Preprint FTI AN UzSSR, Tashkent, 1975; Yad. Fiz. 22, 1168 (1975) [Sov. J. Nucl. Phys. 22, 608 (1976)].
[9]P. L. Jain, B. Girard, *et al.*, Phys. Rev. Lett. 34, 972 (1975).
[10]M. I. Atanelishvili, O. L. Berdzenshvili, *et al.*, Izv. Akad. Nauk SSSR Ser. Fiz. 38, 915 (1974); Pis'ma Zh. Eksp. Teor. Fiz. 18, 490 (1973) [JETP Lett. 18, 288 (1973)] 19, 405 (1971) [JETP Lett. 19, 221 (1974)].
[11]N. Kh. Bostandzhyan, D. T. Bardumyan, G. A. Marikyan, and K. A. Matevosyan, Izv. Akad. Nauk SSSR Ser. Fiz. 38, 912 (1974).
[12]J. Babecki, Acta Phys. Pol. B 6, 443 (1975).
[13]P. R. Vishwanath, A. E. Bussian, *et al.*, Phys. Lett. B 53, 479 (1975).
[14]W Busza, J. E. Elias, *et al.*, Phys. Rev. Lett. 34, 836 (1975).
[15]J. Babecki, Report IFJ No. 911/PH, Cracow, 1976.
[16]Z. Koba, H. B. Nielsen, and P. Olesen, Nucl. Phys. B 40, 317 (1972).
[17]O. M. Kozodaeva, N. V. Maslennikova, *et al.*, Yad. Fiz. 22, 730 (1975) [Sov. J. Nucl. Phys. 22, 377 (1976)].
[18]Zh. S. Takibaev, P. V. Morozova, and N. S. Titova, Yad. Fiz. 20, 392 (1974) [Sov. J. Nucl. Phys. 20, 209 (1975)].
[19]A. A. Goryachikh, Zh. S. Takibaev, N. S. Titova, *et al.*, Yad. Fiz. 13, 1267 (1971) [Sov. J. Nucl. Phys. 13, 729

(1971)].
[20]J. I. Cohen, E. M. Friedlander, *et al.*, Nuovo Cimento Lett. **9**, 337 (1974).
[21]E. M. Friedlander, M. Marcu, and R. Nitu, *ibid.*, p. 341.
[22]Alma-Ata-Leningrad-Moscow-Tashkent collaboration, Yad. Fiz. **19**, 1046 (1974) [Sov. J. Nucl. Phys. **19**, 537 (1974)]; **22**, 736 (1975) [Sov. J. Nucl. Phys. **22**, 380 (1976)].
[23]P. L. Jain, M. Kazumo, *et al.*, Phys. Rev. Lett. 33, 660 (1974).
[24]É. V. Shuryak, Yad. Fiz. **24**, 630 (1976) [Sov. J. Nucl. Phys. **24**, (1976)].
[25]M. I. Adamovich, B. N. Kalinkin, *et al.*, Preprint No. 89, Lebedev Physics Institute, USSR Academy of Sciences, M., 1975.
[26]Alma-Ata-Leningrad-Moscow-Tashkent Collaboration, Contributed Paper at Seventeenth Intern. Conf. on High-Energy Physics, No. 797 (Sec. A2), London, 1974.
[27]B. N. Kalinkin and V. L. Shmonin, Preprint No. R2-7869, Joint Institute for Nuclear Research, Dubna, 1974; Yad. Fiz. **21**, 628 (1975) [Sov. J. Nucl. Phys. **21**, 325 (1975)].
[28]J. W. Martin, J. R. Florian, *et al.*, Nuovo Cimento A **25**, 447 (1975).
[29]J. Babecki, Z. Czachowska, *et al.*, Phys. Lett. B **52**, 247 (1974).
[30]Yu. P. Gorin, S. P. Denisov, *et al.*, Yad. Fiz. 18, 336 (1973) [Sov. J. Nucl. Phys. 18, 173 (1974)].
[31]A. I. Babaev, É. V. Brakhman, *et al.*, Yad. Fiz. 20, 71 (1974) [Sov. J. Nucl. Phys. **20**, 37 (1975)].
[32]P. V. R. Murthy, C. A. Ayre, *et al.*, Nucl. Phys. B 92, 269 (1975).
[33]T. Ya. Inogamova, B. N. Kalinkin, *et al.*, Preprint No. R1-8464, Joint Institute for Nuclear Physics, Dubna, 1974.
[34]É. A. Mamidzhanyan and R. M. Martirosov, Yad. Fiz. 20, 107 (1974) [Sov. J. Nucl. Phys. **20**, 55 (1975)].
[35]Zh. S. Takibaev, I. Ya. Chasnikov, and V. V. Anzon, Preprint No. EVE-10, IFVE AN Kaz. SSR, Alma-Ata, 1974.
[36]S. A. Azimov, A. M. Abdullaev, *et al.*, Izv. Akad. Nauk SSSR Ser. Fiz. 38, 898 (1974).
[37]O. L. Berdzenishvili, D. I. Garibashvili, *et al.*, Izv. Akad. Nauk SSSR Ser. Fiz. 35, 2033 (1971).
[38]I. N. Fetisov, Izv. Akad. Nauk SSSR Ser. Fiz. 35, 2187 (1971).
[39]M. O. Azaryan, S. R. Gevorkyan, and É. A. Mamidzhanyan, Yad. Fiz. **20**, 398 (1974) [Sov. J. Nucl. Phys. 20, 213 (1975)].
[40]J. W. Cronin, Phys. Rev. D 11, 3105 (1975).
[41]D. O. Caldwell, V. B. Elings, *et al.*, Phys. Rev. D 7, 1362 (1973).
[42]W. R. Ditzler, M. Breidenbach, *et al.*, Phys. Lett. B 57, 201 (1975).
[43]J. Eickmeyer *et al.*, Phys. Rev. Lett. 36, 289 (1976).
[44]W. L. Lakin, T. J. Braunstein, *et al.*, Phys. Rev. Lett. 26, 34 (1971).
[45]M. May, E. Aslanides, *et al.*, Phys. Rev. Lett. 35, 407 (1975).
[46]L. B. Bezrukov, V. I. Beresnev, G. T. Zatsepin, *et al.*, Yad. Fiz. 15, 313 (1972) [Sov. J. Nucl. Phys. 15, 176 (1972)].
[47]a) S. Chin, S. Higashi, *et al.*, in: Proc. Thirteenth Intern. Conf. on Cosmic Rays, Denver (1971), p. 1; b) V. V. Borog and A. A. Petrukhin, in: Proc. Fourteenth Intern. Conf. on Cosmic Rays, Munich, 1975, Vol. 6, p. 1949.
[48]N. N. Bingham, Preprint CERN/D, Ph. II/Phys/70-60.
[49]C. Benporad, W. Beusch, *et al.*, Nucl. Phys. B 33, 397 (1974).
[50]R. Arnold, J. P. Engel, *et al.*, Nuovo Cimento A 17, 393 (1973).
[51]A. M. Cnops, F. R. Huson, *et al.*, Phys. Rev. Lett. 25, 1132 (1970).
[52]F. R. Huson, D. J. Miller, *et al.*, Nucl. Phys. B 8, 391 (1968).
[53]V. N. Bolotov, V. V. Isakov, *et al.*, Yad. Fiz. 20, 949 (1974) [Sov. J. Nucl. Phys. 20, 504 (1975)].
[54]A. D. Vasil'kova, M. G. Gornov, *et al.*, Yad. Fiz. 17, 327 (1973) [Sov. J. Nucl. Phys. 17, 166 (1973)].
[55]A. M. Baldin, Issledovaniya s relyativistskimi yadrami v. kn. Materialy 6-i shkoly MIFI po fizike yadra (Investigations Using Relativistic Nuclei, in: Proc. Sixth Nuclear Physics School Held at the Moscow Engineering Physics Institute, 1975).
[56]G. A. Leksin, Yadernyĭ skeĭling (Nuclear Scaling), *ibid.*
[57]A. Dar and J. Vary, Phys. Rev. D 6, 2412 (1972).
[58]V. N. Gribov, Yad. Fiz. 5, 197 (1967) [Sov. J. Nucl. Phys. 5, 138 (1967)].
[59]D. R. O. Morrison, Phys. Rev. 165, 1699 (1968).
[60]R. Glauber, Usp. Fiz. Nauk 103, 641 (1971) [Review Paper at 3rd Internat. Conf. on High-Energy Physics and Nuclear Structure, Columbia University, 1969].
[61]V. M. Kolybasov, v kn. Elementarynye chastitsy (in: Elementary Particles), Atomizdat, M., 1975, No. 1, p. 59.
[62]A. V. Tarasov and Ch. Tsérén, Yad. Fiz. 12, 978 (1970) [Sov. J. Nucl. Phys. 12, 533 (1971)].
[63]A. V. Tarasov and Ch. Tsérén, Preprint No. R2-5604, Joint Institute for Nuclear Research, Dubna, 1971.
[64]S. R. Gevorkyan, V. M. Zhamkochyan, and A. V. Tarasov, Yad. Fiz. **21**, 288 (1975) [Sov. J. Nucl. Phys. **21**, 151 (1975)].
[65]I. M. Dremin and A. M. Dunaevsky, Phys. Rep. C 18, 162 (1975).
[66]E. L. Feĭnberg, Zh. Eksp. Teor. Fiz. 50, 202 (1966) [Sov. Phys. JETP 23, 132 (1966)]; v kn. Problemy teoreticheskoi fiziki sbornik pamyati I. E. Tamma (in: Problems of Theoretical Physics, A collection in Memory of I. E. Tamm), Nauka, M., 1972, p. 248.
[67]E. L. Feĭnberg, v kn. Trudy shkoly molodykh uchenykh Sukhumi (in: Proc. of the Sukhumi School for Young Scientists), Joint Institute for Nuclear Research, Dubna, 1973, p. 56.
[68]A. I. Demianov, V. S. Mursin, and L. I. Sarycheva, in: Proc. Fourteenth Intern. Conf. on Cosmic Rays, Munich, Vol. 7, 1975, p. 2522.
[69]G. T. Zatsepin, Izv. Akad. Nauk SSSR Ser. Fiz. 5, 647 (1962).
[70]I. Ya. Pomeranchuk, Dokl. Akad. Nauk SSSR 78, 889 (1951).
[71]I. L. Rozental' and D. S. Chernavskiĭ, Usp. Fiz. Nauk 52, 185 (1954).
[72]V. S. Barashenkov, A. S. Il'inov, and V. D. Toneev, Yad. Fiz. 13, 743 (1971) [Sov. J. Nucl. Phys. 13, 422 (1971)].
[73]V. S. Barashenkov and S. M. Eliseev, Yad. Fiz. 18, 196 (1973) [Sov. J. Nucl. Phys. 18, 102 (1974)].
[74]K. Gottfried, CERN Preprint TH 1735, 1973.
[75]B. S. Barashenkov *et al.*, Usp. Fiz. Nauk 109, 91 (1973) [Sov. Phys. Usp. 16, 31 (1973)].
[76]L. D. Landau, Izv. Akad. Nauk SSSR Ser. Fiz. **17**, 51 (1953).
[77]I. L. Rozental', Usp. Fiz. Nauk 116, 271 (1975) [Sov. Phys. Usp. 18, 430 (1975)].
[78]Zh. S. Talibaev, Preprint No. 24-75, IFVE AN Kaz. SSR, Alma-Ata, 1975.
[79]S. A. Gurvits, E. I. Daĭbog, and I. L. Rozental', Yad. Fiz. 14, 1268 (1971) [Sov. J. Nucl. Phys. 14, 707 (1972)].
[80]S. É. Belenkin and G. A. Milekhin, Zh. Eksp. Teor. Fiz. 29, 20 (1955) [Sov. Phys. JETP 2, 14 (1956)].
[81]G. A. Milekhin, Zh. Eksp. Teor. Fiz. 35, 1185 (1958) [Sov. Phys. JETP 8, 829 (1959)].
[82]A. A. Emel'yanov, Tr. Fiz. Inst. Akad. Nauk SSSR 29, 169 (1965).
[83]G. A. Milekhin and I. L. Rozental', Zh. Eksp. Teor. Fiz. 33, 197 (1957) [Sov. Phys. JETP 6, 154 (1958)].
[84]E. L. Feĭnberg, Usp. Fiz. Nauk 104, 539 (1971) [Sov. Phys. Usp. **14**, 455 (1972)].
[85]K. Gottfried, Preprint CERN CZNS-260, 1974; Phys. Rev. Lett. 32, 957 (1974).
[86]L. Bertocchi, in: Proc. Sixth Intern. Conf. on High-Energy Phys. and Nuclear Structure, Santa Fe, 1975, p. 238.

[87]E. V. Shuryak, Phys. Lett. B 34, 509 (1971).
[88]F. Cooper, G. Frey, and E. Shonberg, Phys. Rev. Lett. 32, 862 (1974).
[89]E. L. Feĭnberg, in: Proc. Fifth Intern. Colloquium on Collision Multiparticle Hydrodynamics, Leipzig, 1974, p. 789.
[90]V. N. Gribov, Zh. Eksp. Teor. Fiz. 57, 1306 (1969) [Sov. Phys. JETP 30, 709 (1970)].
[91]R. Feynman, Photon-Hadron Interactions, Benjamin, New York, 1972 (Russ. Transl., Mir, M., 1975).
[92]Yu. P. Nikitin and I. L. Rozental', Yad. Fiz. 24, 665 (1976) [Sov. J. Nucl. Phys. 24, (1976)].
[93]A. H. Mueller, Phys. Rev. D 2, 2241 (1970).
[94]B. L. Ioffe, Pis'ma Zh. Eksp. Teor. Fiz. 20, 360 (1974) [JETP Lett. 20, 162 (1974)].
[95]V. N. Gribov, v. kn.: Élementarnye chastitsy, I. Shkola ITEF (in: Elementary Particles, I. ITEF School), No. 1, Atomizdat, M., 1973, p. 65.
[96]E. L. Feĭnberg and D. S. Chernavskiĭ, Usp. Fiz. Nauk 82, 3 (1964) [Sov. Phys. Usp. 7, 1 (1964)].
[97]O. V. Kancheli, Pis'ma Zh. Eksp. Teor. Fiz. 18, 465 (1973) [JETP Lett. 18, 274 (1973)].
[98]V. I. Zakharov and N. N. Nikolaev, Yad. Fiz. 21, 434 (1975) [Sov. J. Nucl. Phys. 21, 227 (1975)].
[99]N. N. Nikolaev, Preprint ITF AN SSSR, Chernogolovka, 1975.
[100]N. N. Nikolaev, Preprint ITF AN SSSR, No. 18, Chernogolovka, 1975.
[101]Yu. D. Bayukov *et al.*, Yad. Fiz. 18, 1246 (1973) [Sov. J. Nucl. Phys. 18, 639 (1974)].
[102]H. G. Baumgardt, J. U. Schott, and E. Schopper, cited in[68], p. 2292.

Translated by S. Chomet